"Dunărea de Jos" University of Galati,

Doctoral School of Mechanical and Industrial Engineering

DOCTORAL THESIS

(Abstract)

GEOMETRIC, KINEMATIC AND DYNAMIC ANALYSIS OF A NEW 6RSS TYPE PARALLEL MECHANISM

PhD. Student,
Eng. LUCIAN MILICA

Scientific coordinator,
Prof. univ. dr. eng. GABRIEL ANDREI

Series I 6: Mechanical engineering No.46
GALAŢI
2018

"Dunărea de Jos" University of Galati,

Doctoral School of Mechanical and Industrial Engineering

DOCTORAL THESIS

(Abstract)

GEOMETRIC, KINEMATIC AND DYNAMIC ANALYSIS OF A NEW 6RSS TYPE PARALLEL MECHANISM

PhD. Student,
Eng. **LUCIAN MILICA**

Committee chairman,	Prof. univ.dr. eng. **IULIAN-GABRIEL BÎRSAN**
Scientific coordinator,	Prof. univ.dr. eng. **GABRIEL ANDREI**
Scientific referrers:	Prof. univ.dr. eng. D.H.C. **ANTON HADĂR** Prof. univ.dr. eng. **DAN SĂVESCU** Prof. univ.dr. eng. **ELENA MEREUȚĂ**

Series I 6: Mechanical engineering No.46
GALAȚI
2018

FOREWORD

Nowadays, for a whole range of applications in different segments of the industry, it is necessary to have the parallel mechanism with six degrees of freedom, which have developed especially in the last fifteen years.

The present paper offers modern and original solutions for the analysis of the workspace, the kinematics and the dynamics of a complex parallel mechanism with six degrees of freedom offering a new perspective for understanding some notions related to these aspects.

Based on multidisciplinary knowledge (mechanisms, mechanics, graphics and computer aided design) as well as practical experience acquired in industry, the research carried out at the Faculty of Engineering at the "Dunărea de Jos" University of Galati is a significant contribution in the field of parallel mechanisms with real implementation perspectives in different areas.

At the end of these three years of scientific activity, I feel honored to address honest thanks and feelings to Prof. Univ. Dr. Eng. Gabriel ANDREI, who, as a scientific coordinator, through the relevant advice and suggestions with a lot of professionalism, contributed to the realization of this paper. Beyond all this, I finally find to discover in the person of the Mr. Professor Gabriel ANDREI a sincere friend but also a mentor who channeled my efforts and energy into the ascending trajectory of my becoming.

Someone said that if you are lucky you meet in life, people how gett attach beyond the words, people who see you more than you see and make the decision to work with you until you'll get to discover that part of you that you're not aware. These people seem to be modeled after your soul. I had the chance to meet such a man in the person of Mr. Lecturer Univ. Dr. Eng. Alexandru NĂSTASE, who through patience, kindness, availability and generosity supported me during the three years of doctoral studies. Thank you, Mr. Professor!

I also thank the teachers at the "Dunarea de Jos" University of Galati: Prof. Univ. Dr. Eng. Laurenţia ANDREI, Senior Lecturer Univ. Dr. Eng. Nicolae DIACONU, Senior Lecturer Univ. Dr. Eng. Doina BOAZU, who contributed with suggestions for improving the paper by participating in supporting the reports.

I would like to thank this way to my wife and daughter for the patience, understanding and unconditional support given during this period.

Galati, 09.05.2018

Eng. Lucian Milica

CONTENTS

FOREWORD **1**

CONTENTS **2**

ABSTRACT **4**

Cap. 1 Particularities of parallel mechanisms and their importance in designing robots with 6 DOF **7**

1.1 Introduction 7
1.2 Advantages of using parallel mechanisms 8
1.3 Kinematic and dynamic analysis 8
1.4 Singular configurations 9
1.5 Redundancy of parallel mechanisms 9
1.6 Workspace volume 9

Cap. 2 Structural model and geometric analysis **11**

of the 6RSS mechanism **11**

2.1 Aspects related to the structure of the mechanisms 11
2.2 General geometric model 12
2.3 Direct geometric model. Restriction method 13
2.4 Inverse geometric model 15
2.5 Translational subspace 16
2.6 The volume of the translational workspace 17
2.7 Orientation subspace 18
2.8 Conclusions on the geometrical modeling of parallel mechanisms 19

Cap. 3 Kinematic analysis of the 6RSS parallel mechanism **20**

3.1 Kinematics particularities of parallel mechanisms 20
3.2 Methods of kinematic modeling 20
3.2.1 Vectorial method 20
3.2.2 Kinematic screw method 21
3.2.3 Partial derivatives method 21
3.3 The kinematic model of the 6RSS parallel mechanisms 22
3.4 Applying the restriction method to determine the kinematic model 23
3.4.1 Applying the kinematic screw method for the 6RSS parallel mechanisms 23
3.5 Generating virtual displacements with Hermite polynomials 24
3.6 Determining the optimal trajectory of the characteristic point with the restriction of avoiding a given space 26
3.6.1 *Determining the optimal path, with the objective function minimizing its travel times* *27*
3.7 Determination of singular configurations of the 6RSS parallel mechanism 29
3.8 Manipulability of parallel mechanism 30
3.9 Conclusions on kinematic analysis and optimization method used 31

Cap. 4 Dynamic analysis of the 6RSS parallel mechanism **32**

4.1 Aspects of the dynamic analysis of the parallel mechanisms 32
4.2 Dynamic model of the 6 RSS parallel mechanism based on the d 'Alembert's principle 33

4.3 Analysis of power losses in spherical joint 35
Cap. 5 General conclusions, original contributions and perspectives 38
5.1 General conclusions 38
5.2 Personal contributions 39
5.3 Research perspectives 40
List of published and presented works 41
References 42

ABSTRACT

Keywords: parallel mechanism, direct geometric model, inverse geometric model, direct kinematic model, inverse kinematic model, singular positions, Jacobian matrix, inverse dynamic model.

This paper highlights aspects of the particularities of parallel manipulators and their importance in the design of the mechanisms with six degrees of freedom, with emphasis being placed on the need to determine the geometric, cinematic and dynamic patterns that allow the final user to manage all the capacities of these.

In the first part the paper presents an actual stage of the researches undertaken in the development of these mechanisms. We highlight the main advantages of using parallel robots in various applications but also their disadvantages. Also presented are the main features of parallel manipulators and methods for improving their performance.

In the second part of the paper we analyze the working space of the new type of manipulator parallel to six degrees of freedom type 6RSS. The parallel manipulator consists of a fixed plate and a mobile platform connected by six independent kinematic chains. Each of the six kinematic chains has an revolute actuator joint and two spherical joints. The general structure of the "*n*" parallel chain mechanism are presented and the customizations done to obtain the parallel mechanism 6RSS type (revolute joint coupler, spherical joint, spherical joint). Was described the method of coordinate transformations in Denavit-Hartenberg notation for one of the parallel chains. The configuration of the mechanism at a given time, ie the position of the effector element, depends on the geometric parameters of the relative positions of the kinematic joints. The two geometric models are detailed: direct model (by which the position of the platform is determined for a set of given angles) and invers model (by which the angle of rotation of one of the motor arms is determined, knowing the position of the platform). Also, applications for the two geometric models are presented.

Analysis of the workspace was done by delimiting the translation subspace (by restricting the platform orientation), by the subspace of the orientations (the characteristic point remains fixed in a given position, restricted by the extreme values of the angles of rotation of the actuated arms).

Determining the geometric model of parallel mechanism is necessary both theoretically and especially in the exploitation of the robot. The multitude of possible positions that the mobile platform can occupy depends both on the variation domains of the independent parameters $\mathbf{q}_j$ and on the structural particularities of the mechanism. The movement of the platform was thus defined by an overlap of two movements: a translation one given by the displacement of the characteristic point and one of the spherical rotation determined by the change of its orientation in relation to a fixed frame. Separating the multitude of mobile platform positions into two three-dimensional spaces (of localizations and orientations) allowed, on the one hand, a more rigorous analysis of the geometrical properties of the parallel mechanism, but also a representation closer to the human perception of the two subspaces.

In the section 3 is presented the kinematic analysis of the parallel mechanism. The kinematic analysis of the parallel mechanism achieve the description of the variation of the scalar parameters of the displacement - between the final and the initial position - in time, without taking into account the forces that intervene during the movement.

Generally the ultimate goal of any robotic application is to achieve a certain technological function, a first requirement being the exact positioning of the end effector at a point or a certain

trajectory. The parallel kinematics study aims to determine the variable parameters associate with each of their joints, so that the coordinates of the end effector element verify a given point in the operating space, while ensuring a certain orientation of it. In this way, relations that define kinematic transformations become kinematic control equations. The kinematic analysis was done by applying the restriction method. The motion equations for the six kinematic chains of the parallel mechanism have been defined when it performs a certain technological function or a movement of the characteristic point on a curve resulting from the intersection of two cylinders. Also, for the same technological function, the kinematic analysis was performed using a CAD software and variations of the angular speeds of the actuating arms was obtained.

On the basis of the kinematic analysis, the movements of the effector element were defined for manipulation operations using polynomial geometric expressions as time functions. It was used the Hermit polynomials function that allow for a permanent follow-up of the movement of the system. Basis on the same Hermite polynomials, a method of optimizing the trajectory of the characteristic point has been developed, with the purpose of minimizing its length and the duration of the trajectory.

Through the kinematic model, the issue of singularities of the parallel manipulator was highlighted. Based on the two Jacobian matrices, the two types of singularities encountered in parallel mechanism were defined. A program was created to make three-dimensional representations of the determinant of functions det[**B**] and det[**A**] of the direct and inverse Jacobian matrix. On the basis of the same program, was represented sections that highlight the critical curves, Also it was possible to establish precisely the existence or the inexistence of the mechanism for a given position and orientation. The resulting diagrams allow the critical configurations to be highlighted and a better understanding of their importance in motion analysis and the programming of such parallel mechanism.

Chapter 4 presents the dynamic analysis of the 6RSS parallel mechanism. Analysis of the dynamic model of parallel mechanism is an important issue for a number of applications in robotics where the effect of inertial forces influences negatively their positioning and orientation.

Determining a dynamic model is a necessary step for controlling the 6 RSS parallel manipulator, as it generally desires a quick response during operation. It should be borne in mind that the mechanism is complex and its dynamic model is difficult to establish. Controlling the parallel real-time mechanism is a real challenge especially if the mobile platform moves at high accelerations. Determining the dynamic model becomes a complicated problem when the inertia forces are applied to the actuators. On the other hand, if the mobile platform performs a certain movement at low speeds and accelerations, the effect of inertial forces may be neglected.

The dynamic model, as well as the other models used in the study of the mechanism, has two complementary practical formulations: the direct dynamic model and the inverse dynamic model.

In the case of the direct dynamic model, the actuating torques $\mathbf{M_a}$ and the inertial characteristics are known and the trajectory, velocity and acceleration of the characteristic point are determined. In the case of the inverse dynamic model, the trajectory, velocity and acceleration of the characteristic point of the final effector is known, and the actuating torques $\mathbf{M_a}$ are determined.

Using the facilities of the *CATIA* program, for the kinematic chain k of the parallel mechanism, the inertial characteristics of its mobile elements for a certain technological function were determined. The inertia matrices of the mobile elements of the mechanism as well as the position, velocities and accelerations of the weight centers of the thirteen mobile elements were determined.

The solution to the dynamic problem of the parallel mechanism was done using the kineto-static method based on d'Alembert's principle, whereby the torque of the reduced inertia forces in the center of mass G of a mechanical system dynamically equilibrates the torque of the applied forces and the connecting forces acting on each S_{jk} element in the system.

Six equivalent kinetostatic equations for the thirteen mobile elements of the 6RSS parallel mechanism were written and resulted in seventy-eight of equations plus six orthogonality equations in a total of eighty-four equations. By solving them, the forces and moments of the kinematic joints have resulted.

Chapter 5 presents the conclusions of the entire research work and highlights personal contributions in the field of geometrical, kinematic and dynamic modeling of parallel mechanism.

Cap. 1 Particularities of parallel mechanisms and their importance in designing robots with 6 DOF

1.1 Introduction

It is well known that parallel manipulators are much stiffer and more accurate than series manipulators [1]. Thus, in recent years, in more technical applications parallel manipulators have been introduced, such as flight simulators, radar antennas, telescopes, pointing devices [2]. In addition, parallel manipulators have also been introduced in the processing centers with multiple degrees of freedom and high speed. Some researchers [3,4] identified as such three types of planar parallel manipulators (Figure 1.1), consisting of three kinematic chains which link the mobile platform with the fixed one.

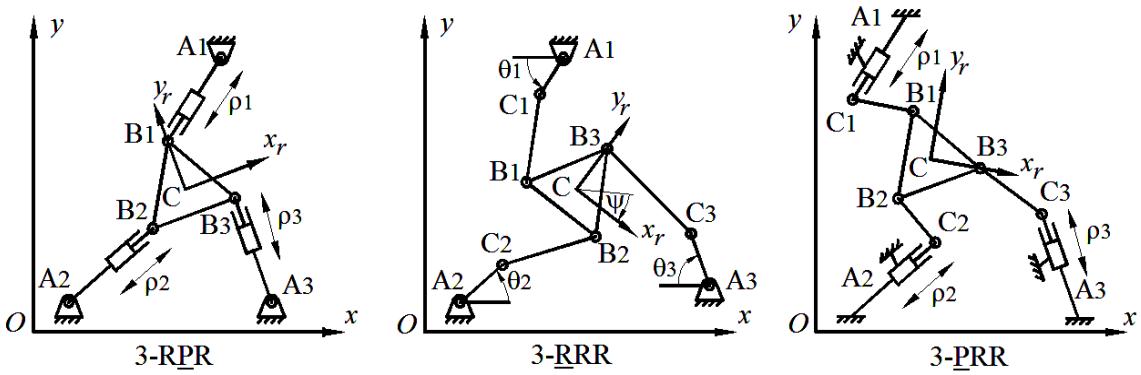

Figure 1. 1 Different types of plane parallel manipulators [3,4].

Jaime Gallardo et al. [5] studied spherical parallel manipulators, making reference to the families of spherical parallel manipulators with two arms. The main characteristic of this family is a compact asymmetric topology consisting of two arms and a spherical joint.

Un manipulator paralel sferic *(SPM)* este un manipulator paralel a cărui platformă mobilă este un element cu punct fix. Astfel toate punctele fixate pe platforma mobilă se deplasează pe sfere concentrice, Di Gregorio [6].

A spherical parallel manipulator is a parallel manipulator whose mobile platform is an element with fixed point. Therefore all points attached to the mobile platform are moving on concentric spheres, Di Gregorio [6]. Several SPM with different architectures have been analyzed in the literature. In their work, Zhang et al. [8], using spherical passive joints along with four connectors, were unable to determine because of redundancy, the only possible orientation of the moving platform. In his work, Wohlhart [9], investigates a displacement analysis of Gough-Stewart platform, where moving the mobile platform is defined by a translation and a rotation movement.

In order to generate a class of spherical joints, Innocenti and Parenti-Castelli [10] have removed three adapters translation, preserving the spherical passive joint, thus connecting the mobile platform with the fixed platform.

Parallel manipulators type RPS (revolute joint-prismatic joint-spherical joint) represent another class of parallel manipulators, which have been dealt with by a number of researchers in different aspects related to the analysis of dynamic and kinematic behaviour [11-13]. A particular approach to kinematic and dynamic problems of the manipulators type RPS is that using the screw theory which proved to be an effective method for determining kinematic characteristics, including instant movements of the mechanism [14-19].

Many researchers sought to explore new approaches that would lead to an increase of the workspace, maximizing mechanism isotropy and avoiding internal singularities [21-23].

The performances of the parallel mechanisms depend to a large extent on their geometry. For designing a parallel mechanism, two criteria are generally considered [24]:
- the performance of the mechanism;
- the final cost.

That is why providing different solutions will allow the end user to choose the best design compromise to solve technical problems [25].

Trajectory planning for parallel manipulators aims to determine a path between the initial and final positions of the effector [26-27]. According to some authors, in the case of parallel mechanisms some restrictions on the characteristic of kinematic chains [28-31] are required.

Using the cylindrical coordinate representation for the Bonev and Ryu workspace [32] determines the dimensions of this space using the MATLAB program for a general parallel manipulator.

1.2 Advantages of using parallel mechanisms

Many applications in precision engineering require high-precision positioning in order to manipulate an object in different environments [33, 34].

For over two decades, parallel robots have attracted the attention of several researchers who consider them to be particularly valuable in terms of alternative construction for robotic mechanisms [35, 36]. Various types of architectures of these mechanisms [37] have recently been studied and many are regularly used in the industrial world, as is the case with different types of machine tools [38] and industrial robots [39].

The accuracy of parallel manipulators was analyzed by various methods that highlighted their performance [40-48].

1.3 Kinematic and dynamic analysis

Mobility is the main parameter of a structural mechanism and also one of the fundamental concepts in modeling dynamic and cinematic mechanisms [49-50].

Grigore Gogu has advanced a new formula for the calculation of mobility parallel mechanisms, with the number of arms $t \geq 2$ [51].

$$M = \sum_{i=1}^{p} f_i - \sum_{i=1}^{t} S_i + S_p; \tag{1.1}$$

Gosselin and Angeles [43] have developed kinematic and dynamic straight model Agile Wrist, which is characterized by three concurrent rotations.

Kinematic analysis is carried out in two ways: via direct kinematic method and by inverse kinematic method. Dynamic analysis of parallel robots is usually approached by the analytical method of classical mechanics [53-56].

In some simplifying hypotheses on the geometry and distribution of robot inertia, Geng et al. [57] and Tsai and Stamper [58] developed a Lagrange equation system of motion.

Starting from the basic equations:

$$\frac{d}{dt}\left(\frac{\partial L}{\partial \dot{\mathbf{x}}}\right) - \frac{\partial L}{\partial \mathbf{x}} + \frac{\partial \mathbf{\Phi}^T}{\partial \mathbf{x}}\boldsymbol{\lambda} = \mathbf{f}; \tag{1.2}$$

Nguyen, Bouzgarrou et al. [59] determines all structural parameters of the robot. Lagrange's analytical calculation is, however, too long and the risk of errors is high [60].

1.4 Singular configurations

Many of the recent work focuses on avoiding critical positions that can handle the mechanism where the workspace is reduced and the problem of finding an algorithm to determine a route that avoids singular configurations becomes complex [61-67].

Two remarkable types of singularities, called direct kinematic singularity and inverse kinematic singularity, are used to study and analyze parallel manipulators [68]. Another approach to the problem of singular positions was highlighted by Zlatanov, Bonev et al. [69], using the screw theory while Wolf, Shoham [70] have investigated these issues through the linear complex approximation. Another way to describe singularities is through geometric line providing a qualitative approach to them [71-73].

Singular positions correspond to the positions in which the Plücker coordinates robot of the axes of the joints form a dependent linear system, and these situations can be characterized in a pure geometric way [74].

The algorithm used for instance, by Stoica A. et al. [75] for the analysis of singular configurations is based on the determinants of the two Jacobian matrixes, [**A**] and [**B**], derived from the geometric model and the inverse geometric model.

The issue of critical positions is the subject of special studies on manipulating mechanisms [76-79]. These studies determine the set of critical positions, which sometimes form "surfaces" in the workspace, thus delimiting the size of this space.

1.5 Redundancy of parallel mechanisms

A new direction of development for the 6 DOF parallel handlers is micro-manipulators. Since 1989, Hara [80] has proposed a 6-SPS parallel micro-manipulator that uses a ceramic piezoelectric actuator. In 1990, Taniguchi [81] developed another 6-PSS parallel micro manipulator. In his work Yuan Yun and Yangmin Li [82] refer to the peculiarities of a parallel manipulator with six degrees of freedom with piezoelectric actuators and double redundancy. The degree of redundancy is the consequence of some particular relative positions of the joint axes [83]. Moreover, according to the latest research, redundancy is a way to avoid single configurations [84].

Redundancy of parallel manipulators is defined as three types: action redundancy, arm redundancy and kinematic redundancy [85-94].

1.6 Workspace volume

The workspace of the robot can be briefly defined as the volume generated by a point of the effector element when the mechanism takes all possible configurations. It can be classified into two categories: reachable workspace and orientation workspace [96].

It is known that an orientation of any system $\{R_1\}$, relative to the other system $\{R_2\}$ is expressed using Euler angles. The final equation of the rotation matrix related to Euler angles is obtained by three successive elementary rotations applied to $\{R_1\}$ system, by angles ϕ, θ and respectively ψ [97].

Using cylindrical coordinate representation for the orientation workspace, Merlet [98], obtains a graph of the volume of this space as a function of angle variation ψ. The volume of the workspace is the subject of a series of scientific researches that underline the importance of this aspect [99-106].

Another problem of parallel mechanisms, in general, is the motion limitation imposed on their kinematic elements in order to avoid any collision between them [107]. Basically, these

limitations determine a restricting workspace and the analysis of positions that may cause such collisions is a prerequisite for the proper functioning of the manipulator (Figure 1. 2).

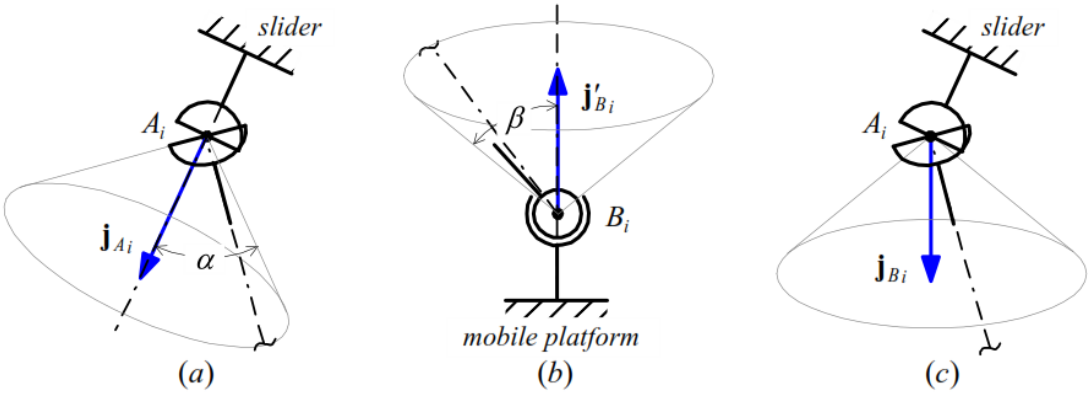

Figure 1. 2 Mechanical limitations imposed on Huck and spherical joints [107].

Cap. 2 Structural model and geometric analysis of the 6RSS mechanism

2.1 Aspects related to the structure of the mechanisms

The mechanism structure is that illustrated in Figure 2.1, with *n* fixed curves (c_1) ... (c_n), n spatial actuators b_1... b_n linked to a mobile platform by n spherical joint, B_1... B_n. The mobile platform is the one enclosed by the B_j points. Links between n spatial actuators b_1 ... b_n and curves (c_1)...(c_n), are achieved through the n-type joints "point on curve" denoted A_1... A_n (Figure 3)..

The degree of mobility of the mechanism is given by Grübler-Kutzbach relationship:

$$M = 6 \cdot m - \sum_{n=1}^{5} c \cdot k_n \; ; \tag{2.1}$$

where:

- c is the joint kinematics class;
- k_n is the number of class n create joints.

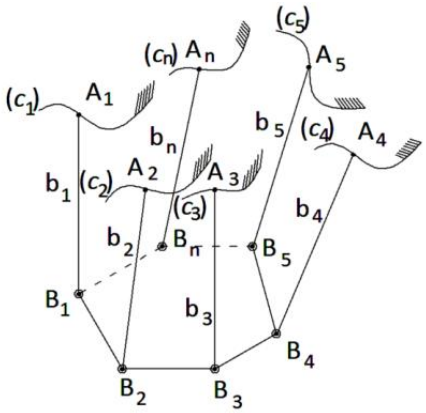

Figure 0. 1 The generic structural scheme of parallel mechanism.

With the mechanical structure of Figure 2, the degree of mobility is:

$$M = 6 \cdot m - \sum_{n=1}^{5} c \cdot k_n = 6 \cdot m - 2k_2 - 3k_3; \tag{2.2}$$

where:

Finally result:

$$M = 6 \cdot (n+1) - 2n - 3n = n + 6;$$

Each actuating arm has a local mobility given by the rotation around the axis $A_j B_j$, which is independent of other possible motions of the mechanism. Eliminating such isolated mobility, it results $M = 6$.

This paper presents the approach to the workspace of the mobile platform of a RSS type manipulator with six degrees of freedom in different situations, when the constraints imposed on the platform are fully determined, limited or nonexistent. The mechanism has the following features:

1. axis of rotational active joints Δ_j that generate circular trajectories (c_j) are coplanar, two-by-two coincident and central-symmetrically disposed ;
2. the actuating arms r_j are of equal length;
3. l_j rods are of equal length;
4. spherical joints of the mobile platform are coplanar and their centers are located on the vertices of a regular hexagon;

5. the distance between A'_j and A'_{j+1} is equal to the distance between B_j and B_{j+1}, $j = 1, 3, 5$. A'_j and A'_{j+1} are projections of points A_j and A_{j+1}on the corresponding axis of the actuated joint.

The 6RSS parallel manipulator consists of a fixed plate, to which six actuators are fitted, and a mobile platform on which is fitted the seventh actuator to drive a milling tool (Figure 2. 2). The components that transmit the movement to the mobile platform are six branches driven by the six actuators.

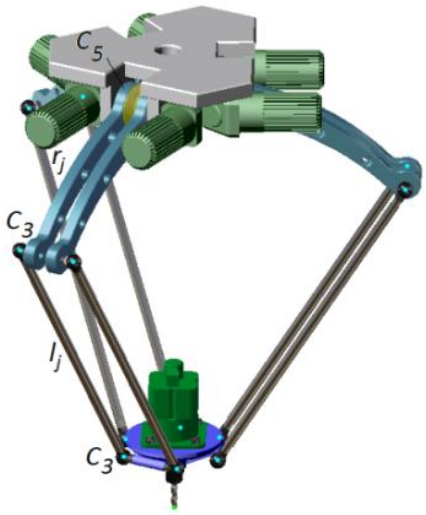

Figure 0. 2 The new parallel manipulator 6RSS, highlighting kinematic joints.

2.2 General geometric model

The set of positions of mobile platform resulted when the six actuating arms cover their entire motion domain is a subset of the *task space*, which has six dimensions. From a practical viewpoint, it is useful to separate the *task space* into two spaces with three dimensions: localization space, and orientation space.

The geometrical properties of the 6RSS manipulator are described by the direct geometric model or inverse geometric model.

Direct geometric modeling consists of assigning values of the θ_1^k of each kinematic chain *k*, then determining the other parameters $\theta_2^k,\ldots,\theta_6^k, x, y, z, \alpha, \beta, \gamma$ corresponding to each kinematic chain. The calculation is reduced to a multiple matrix product, and the orientation and localization parameters of the effector element are read directly from the resulting product matrix. There will be a system of six linear equations of the form:

$$S = \begin{cases} \mathbf{A}_{1,0}^1 \cdot \mathbf{A}_{2,1}^1 \cdot \mathbf{A}_{3,2}^1 \ldots \mathbf{A}_{6,5}^1 = \mathbf{B_1} \\ \cdot \\ \cdot \\ \cdot \\ \mathbf{A}_{1,0}^6 \cdot \mathbf{A}_{2,1}^6 \cdot \mathbf{A}_{3,2}^6 \ldots \mathbf{A}_{6,5}^6 = \mathbf{B_6} \end{cases}; \tag{2.3}$$

in which:

$$\mathbf{B} = \mathbf{T}_{O,B}^{-1} \cdot \mathbf{T}_{P,B} \cdot \mathbf{T}_{P,6}^{-1}; \tag{2.4}$$

By solving this system of equations with thirty-six unknowns we determine the working space of the parallel manipulator for any angular variation θ_1^k of the actuators l_1^k.

Invers geometric modeling consists of the algebraic assembly by which, starting from a given position of the mobile platform in the operative space, the Lagrange parameter values corresponding to that position can be determined.

2.3 Direct geometric model. Restriction method

În Figure 2. 3 schematically illustrates the general case of one of the kinematic chain of the 6RSS parallel manipulator, with six rotational joints O_k and twelve spherical joints, in A_k point and B_k point respectively. The actuating arms r_k are rotated with θ_1^k angle arround the axis with unit vector $\mathbf{u_k}$, which passes through the O_k point. The position of the O_k point in the $\{R_b\}$ reference system is known and both the length of the actuating arms r_k and the value of the angle θ_1^k are also known. By using parameters (O_k, r_k, θ_1^k), we can easly determine the centre position of the A_k spherical joint (k =1 … 6). Between B_k coordinates of A_kB_k elements and b_k coordinates of the mobile platform it is the relation:

$$\{B_k\}=\left[\mathbf{T}_{P,B}\right]\cdot\{b_k\}; \tag{2.5}$$

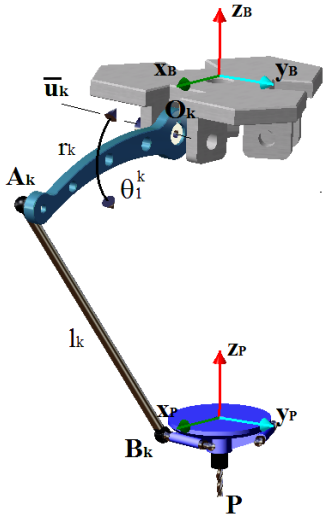

Figure 0. 3 Structural 3D model of a single kinematic chain of the 6RSS manipulator.

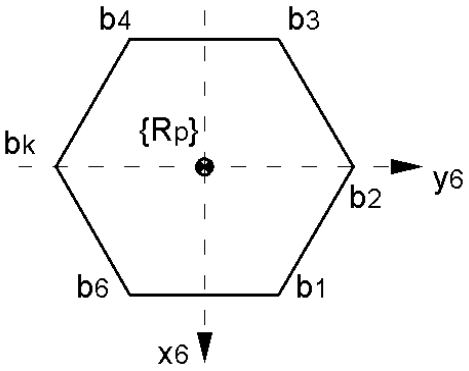

Figure 0. 4 Mobile platform of the parallel manipulator.

In Figure 2.4 it is represented the mobile platform of the parallel manipulator. The platform has a polygonal shape and the intersection of its sides determines the b_1... b_k points. The b_k point has the coordinate $b_{k,1}$, $b_{k,2}$, $b_{k,3}$ in the $\{R_P\}$ reference system of the platform. x_A, y_A and z_A are functions of θ_k and x_B, y_B, z_B are the coordinates of B_k points in the fixed reference system.

The geometric direct model for the 6RSS new manipulator is given by the equation system (2.6). The system allows to determine *x, y, z, α, β, γ* parameters of each *k* kinematic chain for the known θ_j^k parameters of the mechanism.

$$S = \begin{cases} (x_B^1 - x_A^1)^2 + (y_B^1 - y_A^1)^2 + (z_B^1 - z_A^1)^2 - l^2 = 0 \\ \cdot \\ \cdot \\ \cdot \\ (x_B^6 - x_A^6)^2 + (y_B^6 - y_A^6)^2 + (z_B^6 - z_A^6)^2 - l^2 = 0 \end{cases}; \quad (2.6)$$

Doing notation for the left member of (2.6) with $f_k\ (x, y, z, \alpha, \beta, \gamma)$, equation system can be written as:

$$S = \begin{cases} f_1(x, y, z, \alpha, \beta, \gamma) = 0 \\ \cdot \\ \cdot \\ \cdot \\ f_6(x, y, z, \alpha, \beta, \gamma) = 0 \end{cases}; \quad (2.7)$$

where, the unknowns $x, y, z, \alpha, \beta, \gamma$ can be found in partial derivative equations of system (2.6). This equation system can be solved by Newton method.

2.3.1 Application to the direct geometric model

Based on the direct model, a program highlighting the convergence of the intermediate solutions was developed for the calculation of the parameters $x, y, z, \alpha, \beta, \gamma$. The program interface is shown in Figure 2.5.

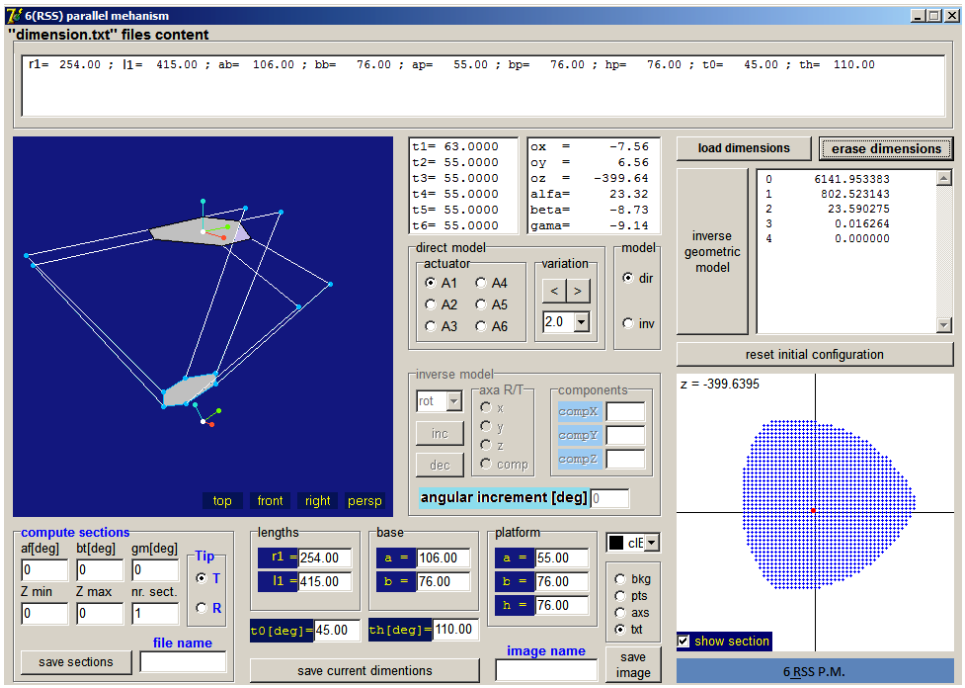

Figure 0. 5 Interface of the simulation program.

We can distinguish the typical dimensions of the 6RSS parallel manipulator, values of the angles $\theta_k\ (k = 1 \ldots 6)$ and the parameters $x, y, z, \alpha, \beta, \gamma$ which describe the location and the orientation of the mobile platform.

We have noted with $A_1 \ldots A_6$ the six actuators and a set of values for which the angular variation was established. We also represented a horizontal section through the volume described by the reachable positions of the mobile platform at same point. Also, the interface contains a text box with information on the number of iterations i, the error values of ε and a schematic representation of the 6RSS parallel manipulator, with multiple possibilities of viewing it from different angles. For a given position of the actuating arms we get different sections of the robot workspace.

2.4 Inverse geometric model

Determination of the inverse geometric model was done by a geomeric construction. Developed equations represent an algebraic transposition of this construction. In the following section, a sequence of geometric constructions to determine the angular parameter δ for one actuating arm will be described. In contrast to the direct model, in case of an inverse model, the six parameters δ_j $(j = 1 \dots 6)$ can be determined independently, therefore the algorithm refers only to one branch of the parallel mechanism.

Let us consider a Cartesian coordinate system of unit vectors $(\mathbf{v}, \mathbf{u}, \mathbf{k})$ attached to the cylindrical articulation *C*, in which $\mathbf{u}$ is the unit vector of the articulation axis, $\mathbf{k}$ is parallel to fixed axis z_0 of the reference system (x_0, y_0, z_0) and $\mathbf{v} = \mathbf{u} \times \mathbf{k}$.

The geometrical sequence of the inverse geometrical model includes the following steps:

1. Calculating the coordinates of point *B* using the equation:

$$\mathbf{r}_B = \mathbf{T}_{P,O} \cdot \mathbf{b}; \tag{2.8}$$

where $\mathbf{b}$ is the vector of the local coordinates (in the platform reference frame) of point *B*.

2. Determining the distance d between point *B* and plane $[\mathbf{k}, \mathbf{v}]$:

$$d = (\mathbf{r}_B - \mathbf{r}_C) \cdot \mathbf{u}; \tag{2.9}$$

If $|d| \geq l_1$ jump out to point 6.

3. Calculating the coordinates of point *B*':

$$\mathbf{r}_{B'} = \mathbf{r}_B - d \cdot \mathbf{u}; \tag{2.10}$$

4. Calculating the distances $a = B'C$ and $r = B'A$ with relations:

$$a = |\mathbf{r}_C - \mathbf{r}_{B'}| \text{ and } r = |\mathbf{r}_A - \mathbf{r}_{B'}|; \tag{2.11}$$

If $a \geq r + r_1$ or $a \leq r - r_1$ jump out to point 6.

5. Calculating the value of angle φ (determined by the vectors **v** and **CB′**) projecting vector **CB′** on the unit vectors $\mathbf{k}$ and $\mathbf{v}$.

Resolving AB'C triangle (Figure 2.7) and determining angle between vectors **AB** and **CB′**). Obtaining the solution $\delta = \varphi - \tau$. End of sequence.

6. There is no solution. End of sequence.

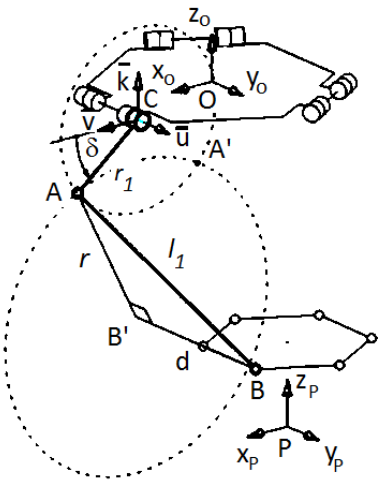

Figure 0. 6 Representation of a kinematic chain of the parallel manipulator 6RSS.

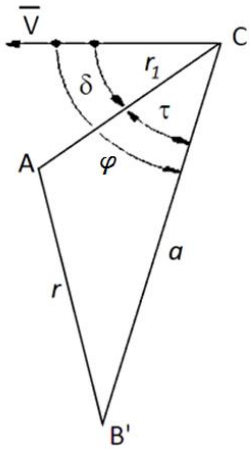

Figure 0. 7 Highlighting of the angles φ, δ and τ.

Point *A* is at the same time on the circle plane determined by the unit vectors $\mathbf{k}$ and $\mathbf{v}$, with radius r_1 centered on *C* and on the sphere of center *B* and radius l_1 (Figure 2.6).

2.5 Translational subspace

Due to the particular structure of the 6RSS parallel manipulator, the set of platform positions determines a space with six dimensions. Figure 2.8 shows cross-sections through a plane normal to the axis of rotation of the arm.

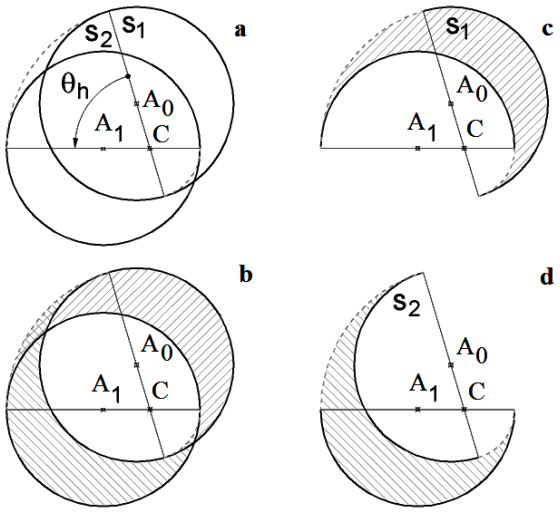

Figure 0. 8 Cross-sections through locus of B_k point.

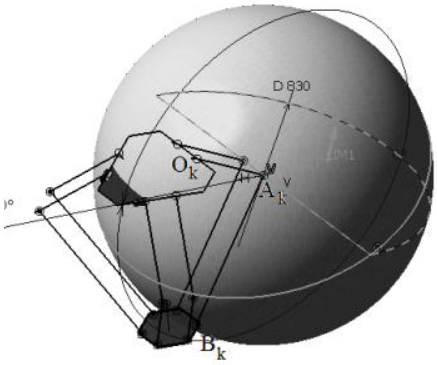

Figure 0. 9 Spherical surface generated by locus of point B_k.

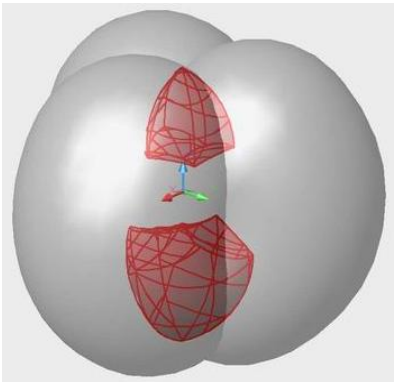

Figure 0. 10 Volume translated with the $\mathbf{B_kP}$ vector.

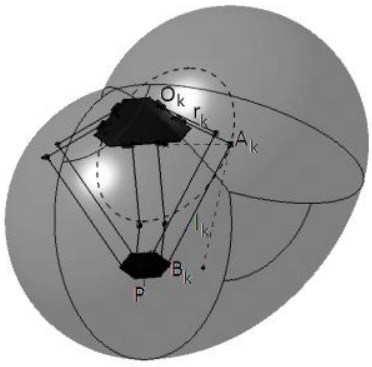

Figure 0. 11 The volume when the sphere is moving on circle arc with radius r_k.

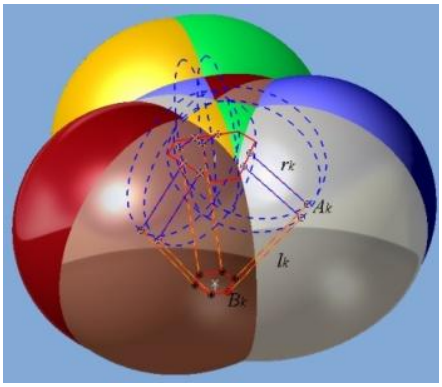

Figure 0. 12 The six individual loci before translation.

For a given position of the actuatuatig arm, the locus of point B_k will be the spherical surface of radius $l_1 = A_kB_k$ and center A_k (Figure 2.9). For a single kinematic chain, the obtained volume can be viewed in Figure 2.11.

Since the platform is simultaneously affected by the restrictions applied to the six parallel chains, the locus of point *P* of the platform (reachable workspace of the point *P*) will be the intersection of the six individual loci described previously (Figure 2.12), respective translating the volume with the vector $\mathbf{B_kP}$ (Figure 2.10).

The practical determination of the tangible space under the specified conditions was done with an AutoLISP application under AutoCAD and a Catia application, using the ability of the respective programs to generate volumes and intersect them.

Using the same AutoLISP application, we can determine the tangible space of the 6RSS parallel mechanism for different combinations of parameters a_1, b_1, a_2, b_2, r_1, l_1, h.

An extremely important role in achieving the largest possible volume of the tangible space of the robot has the parameter a_1. A smaller influence on tangible volume has the parameter a_2, whose variation does not cause major changes to it.

2.6 The volume of the translational workspace

An algorithm has been developed to determine the boundaries of the technological space in order to maximize its volume.

To illustrate how to use the proposed algorithm, a program in AutoLISP was written through which sections were done, and the $V_{(z)}$ diagram was realised. For this, a 'scanning' section procedure was written, determining the distance ''y'' at which the area of the rectangle entered is the maximum (Figure 2.13).

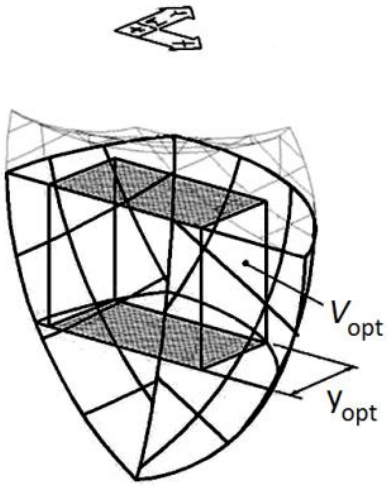

Figure 0.13 Determining the rectangle of maximum area

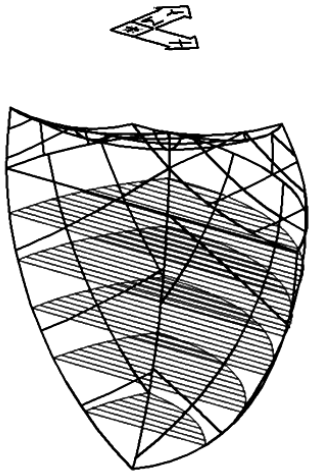

Figure 0. 14 Equidistant sectioning of the reachable workspace

Next, a program was created to realised equidistant tangential sectioning with a large number of planes, and each of these had the procedure described above (Figure 2.14).

In the diagram of Figure 2.15 is the solution of the resulting maxim-maximorum volume.

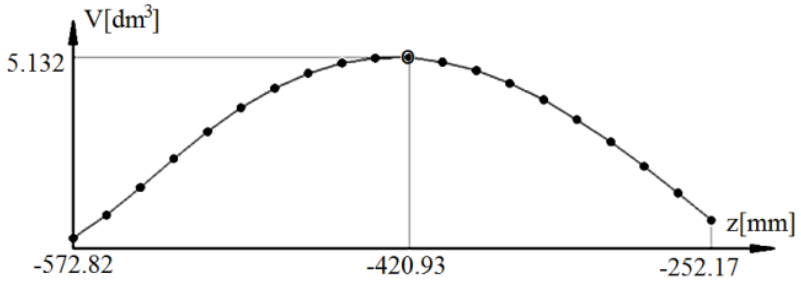

Figure 0. 15 Volume chart and the maximum-maximorum value

2.7 Orientation subspace

As mentioned before in this work, for a certain position of the characteristic point given by the Cartesian coordinates x, y, z there is a tridimensional representation of possible orientations of the mobile platform given by the angular coordinates α, β, γ.

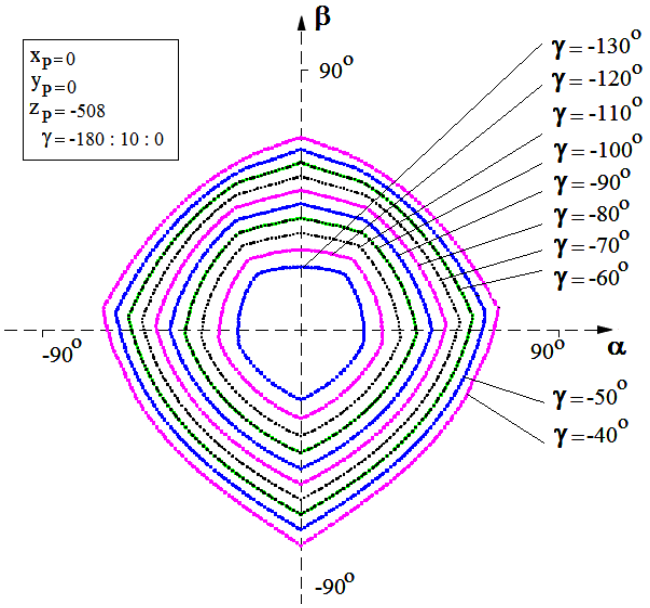

Figure 0. 16 Sections through orientation subspace for point *P* (0, 0, -508)

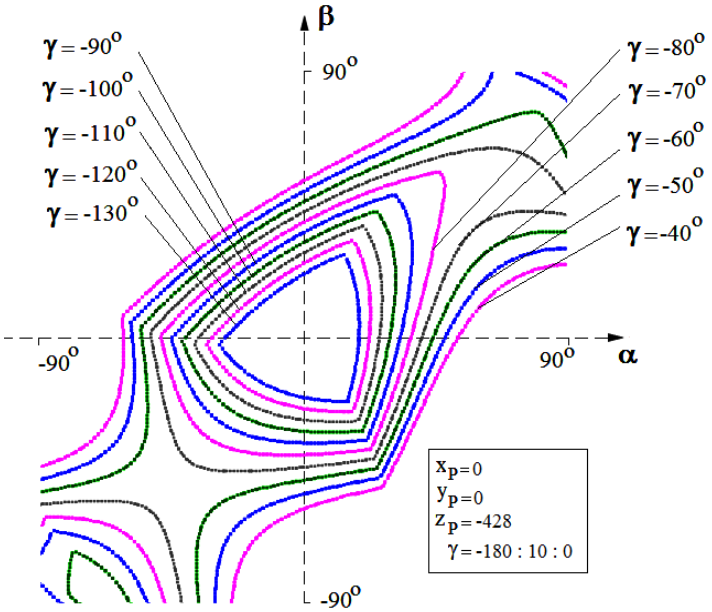

Figure 0. 17 Sections through orientation subspace for point *P* (0, 0, -428)

The angles of variation α, β, γ are determined based on the rotation restrictions of the actuating arms. Based on original computer programs, we obtained cross-sections through parallel planes of the three-dimensional space.

It has been highlighted sections through this orientation subspace. Thus, for a some position of characteristic point *P*, doing a section to an certain *γ* we can see from the top view the contour of the surface for the respective section (Figure 2. 16 - 2. 17).

This contour bounds the set of values that can be assigned for *α* and *β*. In other words, for any values of *α* and *β* outside of the contour *γ*, the manipulator orientation is not possible.

2.8 Conclusions on the geometrical modeling of parallel mechanisms

Determining the geometric model of parallel mechanisms is necessary both theoretically and especially in the exploitation of the robot. The motion of the platform is defined by an overlap of two movements: a translation one given by the displacement of the characteristic point and a spherical rotation determined by the change of its orientation towards a fixed reference sistem.

Separating the subset of mobile platform positions into two three-dimensional spaces (locations and orientations) thus allows for a more rigorous analysis of the geometrical properties of the parallel mechanism, but also for a closer representation of the human perception of the two spaces.

The use of the inverse geometric model and the translation subspace allowed the development of computational algorithms and software applications to determine the optimum workload of a parallel manipulator type 6RSS. The method used to determine the technological workspace is useful in determining the working performance of the manipulators parallel to the chosen structure and can be extrapolated and in the modeling of other structural schemes.

Using the algorithm used to determine the extreme values of the technological space, we can achieve its optimization, thus providing a better understanding of the possibilities of exploiting the parallel mechanism under consideration. Determining the dimensions of the technological space as accurately as possible determines the limits between which kinematic parameter values can be controlled.

Cap. 3 Kinematic analysis of the 6RSS parallel mechanism

3.1 Kinematics particularities of parallel mechanisms

An important advantage of parallel manipulators is that superior structural stiffness makes them preferable to serial machines when handling heavy loads or performing high precision machining [109-113]. Parallel mechanisms also have a better distribution of inertia and are capable of performing accurate and fast movements.

These qualities make parallel mechanisms find their applicability in various fields: flight simulators and fine positioning devices and fast packing for high-speed milling machines [114,115].

Various solutions for modeling the inverse Jacobian used in expressing speeds are presented in the literature [116-123].

3.2 Methods of kinematic modeling

3.2.1 Vectorial method

The characterization of the manipulators in terms of the transformation of the relative movements of the actuating joint in the movement of the effector element is done by their kinematic model. Considering a mechanism with n movable elements, it is known that the generalized velocity vector has the form:

$$\dot{\mathbf{q}}_{\mathbf{1}} = [\dot{q}_1 \ \dots \ \dot{q}_n]; \tag{3.1}$$

Let be a mobile *xOyz* coordinate system originated at point *O*, **OP** being the position vector of a point *P* (belonging to the S-body) to the origin of the system and $\mathbf{v}_O$ the linear velocity of point *O* (Figure 3.1). We also define the vector $\mathbf{v}_P$ as the point *P* speed.

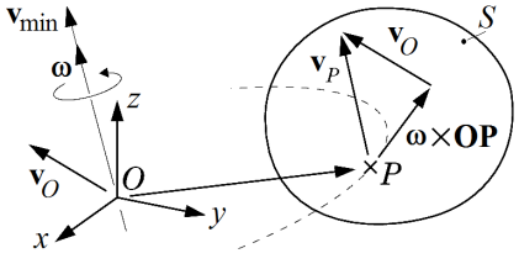

Figure 3.1 Components that determine speed of the body [124].

The motion of the rigid consists of a translation in the direction of $\mathbf{v}_O$ and a rotation with the velocity $\boldsymbol{\omega}$ around an axis passing through the point *O*. Between the four vectors there is the Euler relation:

$$\mathbf{v}_P = \mathbf{v}_O + \boldsymbol{\omega} \times \mathbf{OP}; \tag{3.2}$$

Angular velocity $\boldsymbol{\omega}$ is located on a straight line called roto-translation axis in the same direction as the minimum speed $\mathbf{v}_{\min}$ of the points on this axis.

Let be $\mathbf{i}, \mathbf{j}, \mathbf{k}$ unit versor of the axis x, y, z. We can express $\boldsymbol{\omega}$ and $\mathbf{v}_O$ vectors in Cartesian coordinates:

$$\boldsymbol{\omega} = \omega_x \cdot \mathbf{i} + \omega_y \cdot \mathbf{j} + \omega_z \cdot \mathbf{k}; \tag{3.3}$$

$$\mathbf{v}_O = v_{Ox} \cdot \mathbf{i} + v_{Oy} \cdot \mathbf{j} + v_{Oz} \cdot \mathbf{k}; \tag{3.4}$$

The six coordinates $\omega_x, \omega_y, \omega_z, v_{Ox}, v_{Oy}, v_{Oz}$ are known as the Plücker coordinates. Thus, the movement of the body can be determined as a sum of elementary movements; three translations after the three axes and three turns along the same axes.

3.2.2 Kinematic screw method

Determining the kinematics of parallel mechanisms involves establishing the equations of the resultant motion of a rigid body having a relative motion in relations to a mobile coordinates system. The resultant movement can be represented trough the kinematic screws by composing the screws of all the components in motion.

In Figure 3.2 we have attached to a rigid body a coordinate system with center in point *P* (identical to the origin of the system *O*) which belongs to this.

Consider the rigid body in an instantaneous motion relative to a roto-translational axis (Δ). **ω** is the angular velocity of the body, **r** is the distance from point *P* relative to the roto-translational axis (Δ) and λ is the screw parameter given by the relation:

$$\lambda = \frac{\mathbf{v}_{\min}}{\omega}; \tag{3.5}$$

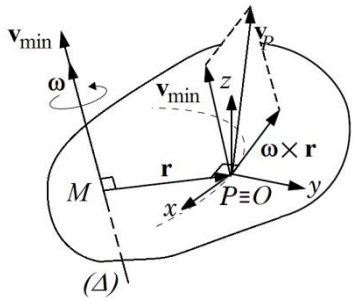

Figure 3. 2 Elements of the kinematic screw.

We have the following expressions:

$$\boldsymbol{\omega} = \omega \cdot \mathbf{u}; \tag{3.6}$$

$$\mathbf{w} = \mathbf{r} \times \mathbf{u} + \lambda \cdot \mathbf{u}; \tag{3.7}$$

where **u** is the unit vector of the instantaneous axis of rotation.

When this axis is even one of the axes of the reference system, the expressions of the unit vector $\mathbf{u_x}$, $\mathbf{u_y}$, $\mathbf{u_z}$ of the homologous axes result slightly.

Thus, any movement may be characterized by an overlap of two elementary movements : translational movement by **u** direction and a rotational movement. The expression of the kinematic screw becomes:

$$\boldsymbol{\Omega} = \boldsymbol{\Omega}_{\text{rot}} + \boldsymbol{\Omega}_{\text{tra}} = \begin{bmatrix} \boldsymbol{\omega} \\ \mathbf{r} \times \boldsymbol{\omega} \end{bmatrix} + \begin{bmatrix} \mathbf{0} \\ \mathbf{v} \end{bmatrix}; \tag{3.8}$$

3.2.3 Partial derivatives method

The differential model of a robot is the one that allows the differential calculation of the dx of the operational coordinates defining the position in the work space, depending on the differential dq of the generalized coordinates associated with each mechanical joint. Analytically, this dependence can write:

$$dx = [\mathbf{J}] \cdot dq; \tag{3.9}$$

where $[\mathbf{J}]$ is the global Jacobian matrix which has the expression:

$$[\mathbf{J}] = [\mathbf{A}]^{-1} \cdot [\mathbf{B}]; \tag{3.10}$$

and the matrices [**A**] and [**B**] represent the inverse Jacobian, respectively the direct Jacobian of the mechanism.

For most parallel mechanisms, it is more convenient to determine the Jacobian matrix that is related to the inverse transformation given by expression:

$$[\mathbf{J}]^{-1} = [\mathbf{B}]^{-1} \cdot [\mathbf{A}]; \tag{3.11}$$

The general kinematic model of the parallel mechanism is given by the relation:

$$[\mathbf{B}] \cdot [\dot{\mathbf{q}}] = [\mathbf{A}] \cdot [\dot{\mathbf{w}}]; \tag{3.12}$$

The direct kinematic model is the transformation by which instantaneous movement of the end effector element can be determined as a function of the relative speeds of the actuating joints:

$$\begin{bmatrix} \mathbf{v_P} \\ \boldsymbol{\omega} \end{bmatrix} = [\dot{\mathbf{w}}] = [\,\mathbf{J}] \cdot [\dot{\mathbf{q}}]; \tag{3.13}$$

Where $\mathbf{v_P}$ represent the velocity vector of the characteristic point having the expression: $[\mathbf{v_P}]^{\mathbf{T}} = [v_{Px} \quad v_{Py} \quad v_{Pz}] = [\dot{\mathbf{x}} \quad \dot{\mathbf{y}} \quad \dot{\mathbf{z}}]$ and $[\boldsymbol{\omega}]^{\mathbf{T}} = [\omega_\alpha \quad \omega_\beta \quad \omega_\gamma] = [\dot{\alpha} \quad \dot{\beta} \quad \dot{\gamma}]$. α, β, γ represent Euler angle in the Roll-Pitch-Yaw system.

3.3 The kinematic model of the 6RSS parallel mechanisms

The 6RSS parallel mechanisms schematically represented in Figure 3. 3 has a fixed plate (on which the six drive actuators are mounted) and a mobile platform on which is mounted a seventh servomotor acting a milling tool.

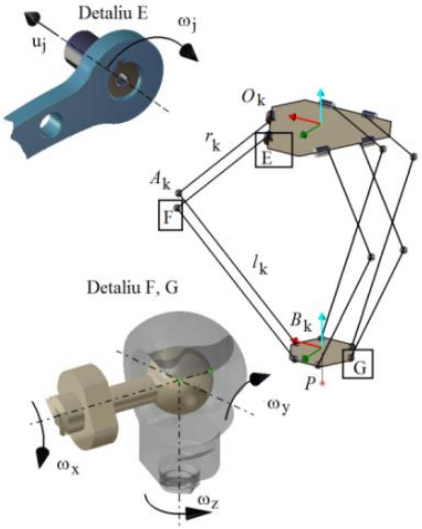

Figure 3. 3 Schematic representation of mechanism 6 RSS.

The parallel mechanism is represented in Figure 3.4 in 3D view and in Figure 3.5 is the kinematic scheme of one the six kinematic *k* chains.

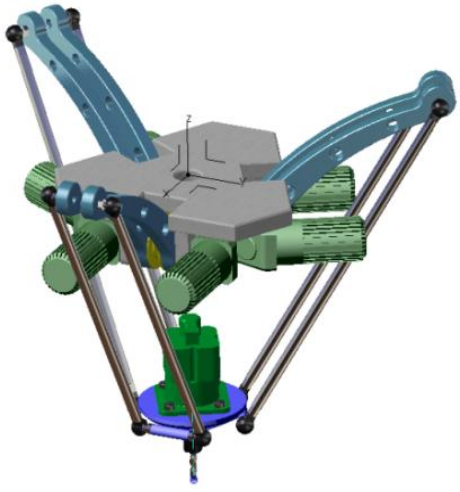

Figure 3. 4 The new 6RSS parallel mechanisms.

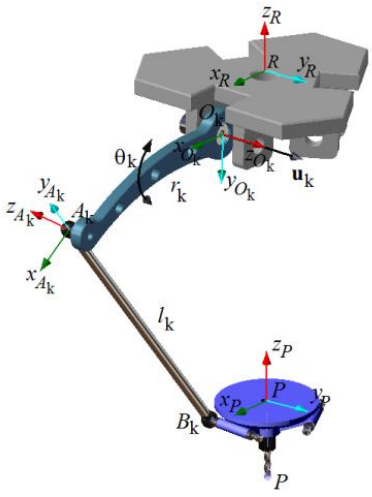

Figure 3. 5 The kinematic scheme of one branch.

Starting from the kinematic scheme presented above, we will define the motion equations for the six kinematic chains of the parallel mechanism when the characteristic point *P* follows a spatial curve (*C*) resulting from the intersection of two cylinders with radius $r_1 = 200\ \text{mm}$ and the center at point $Q_1\ (200, -100, -500)$, respectively $r_2 = 75\ \text{mm}$ and the center at point $Q_2\ (0, 0, -500)$.

3.4 Applying the restriction method to determine the kinematic model

The position of the platform is determined by the position of point *P* and the angle α (rotation of the platform by the axis of the cylinder).

We will begin to write the motion equations for one of the kinematic chains, for the other chains the calculations are analogous.

$$S = \begin{cases} \mathbf{v_{A_1}} = \boldsymbol{\omega_1} \times \mathbf{O_1A_1} \\ \mathbf{v_{B_1}} = \mathbf{v_P} + \boldsymbol{\omega_P} \times \mathbf{PB_1} \end{cases}; \tag{3.14}$$

It is known that:

$$\boldsymbol{\omega_1} = \omega_1 \cdot \mathbf{u_{12}}; \tag{3.15}$$

From relations (3.35) and (3.36) it results:

$$S = \begin{cases} \mathbf{v_{A_1}} = \omega_1 \cdot \mathbf{u_{12}} \times \mathbf{O_1A_1} \\ \mathbf{v_{B_1}} = \mathbf{v_P} + \boldsymbol{\omega_P} \times \mathbf{PB_1} \end{cases}; \tag{3.16}$$

For the six kinematic chains, we will have to solve six equations of form (3.17) whose matrix representation is:

$$\begin{bmatrix} q_1 & 0 & 0 & 0 & 0 & 0 \\ 0 & q_2 & 0 & 0 & 0 & 0 \\ 0 & 0 & q_3 & 0 & 0 & 0 \\ 0 & 0 & 0 & q_4 & 0 & 0 \\ 0 & 0 & 0 & 0 & q_5 & 0 \\ 0 & 0 & 0 & 0 & 0 & q_6 \end{bmatrix} \cdot \begin{bmatrix} \omega_1 \\ \omega_2 \\ \omega_3 \\ \omega_4 \\ \omega_5 \\ \omega_6 \end{bmatrix} = \begin{bmatrix} a_1 & b_1 & c_1 & s_1 & r_1 & t_1 \\ \vdots & & & & & \vdots \\ \vdots & & & & & \vdots \\ \vdots & & & & & \vdots \\ \vdots & & & & & \vdots \\ a_6 & b_6 & c_6 & s_6 & r_6 & t_6 \end{bmatrix} \cdot \begin{bmatrix} v_{P_x} \\ v_{P_y} \\ v_{P_z} \\ \omega_{P_x} \\ \omega_{P_y} \\ \omega_{P_z} \end{bmatrix}; \tag{3.17}$$

The relationship (3.17) written in compact form becomes:

$$[\mathbf{B}] \cdot [\dot{\mathbf{q}}] = [\mathbf{A}] \cdot [\boldsymbol{\tau}];$$

In order to determine the components of the vector $\boldsymbol{\omega_P}$, we consider the particularity of the application, i.e. the platform has a rotation motion with α angle, the components on the other two directions being null.

3.4.1 Applying the kinematic screw method for the 6RSS parallel mechanisms

In the case of the parallel mechanism analyzed, by composed a number of kinematic screws of a kinematic chain, the resulting motion will be described by the kinematic screw obtained by summing the *n* kinematic screws:

$$\boldsymbol{\Omega} = \boldsymbol{\Omega}_1 + \boldsymbol{\Omega}_2 + \cdots + \boldsymbol{\Omega}_n; \tag{3.18}$$

Each actuated arm has a local mobility given by the rotation around the axis A_kB_k, independent movement relative to the other possible movements of the mechanism (Figure 3.6).

At each angular velocity $\boldsymbol{\omega_1}, \ldots, \boldsymbol{\omega_P}$ corresponds a kinematic screw $\boldsymbol{\Omega}_1, \ldots, \boldsymbol{\Omega}_P$ so that for the six kinematic chains of the mechanism will result the system of equations:

$$\begin{cases} \boldsymbol{\Omega_1^{(1)}} + \boldsymbol{\Omega_2^{(1)}} + \cdots + \boldsymbol{\Omega_6^{(1)}} = \boldsymbol{\Omega_P} \\ \boldsymbol{\Omega_1^{(2)}} + \boldsymbol{\Omega_2^{(2)}} + \cdots + \boldsymbol{\Omega_6^{(2)}} = \boldsymbol{\Omega_P} \\ \boldsymbol{\Omega_1^{(3)}} + \boldsymbol{\Omega_2^{(3)}} + \cdots + \boldsymbol{\Omega_6^{(3)}} = \boldsymbol{\Omega_P} \\ \boldsymbol{\Omega_1^{(4)}} + \boldsymbol{\Omega_2^{(4)}} + \cdots + \boldsymbol{\Omega_6^{(4)}} = \boldsymbol{\Omega_P} \\ \boldsymbol{\Omega_1^{(5)}} + \boldsymbol{\Omega_2^{(5)}} + \cdots + \boldsymbol{\Omega_6^{(5)}} = \boldsymbol{\Omega_P} \\ \boldsymbol{\Omega_1^{(6)}} + \boldsymbol{\Omega_2^{(6)}} + \cdots + \boldsymbol{\Omega_6^{(6)}} = \boldsymbol{\Omega_P} \end{cases}; \tag{3.19}$$

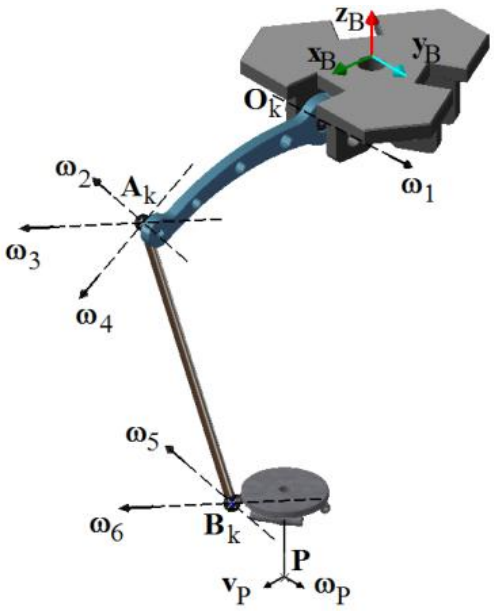

Figure 3. 6 Angular velocities of kinematic joints belonging to a *k*-chain.

We get the expressions of ω_P , λ_P and $\mathbf{r_P}$ that fully describe the movement of the platform:

$$\omega_P = \sqrt{\left(\Omega_1^{\mathrm{P}}\right)^2 + \left(\Omega_2^{\mathrm{P}}\right)^2 + \left(\Omega_3^{\mathrm{P}}\right)^2}; \tag{3.20}$$

$$\lambda_P = \Omega_1^{\mathrm{P}} \cdot \Omega_4^{\mathrm{P}} + \Omega_2^{\mathrm{P}} \cdot \Omega_5^{\mathrm{P}} + \Omega_3^{\mathrm{P}} \cdot \Omega_6^{\mathrm{P}}; \tag{3.21}$$

$$\mathbf{r_P} = \left(\Omega_1^{\mathrm{P}} \cdot \mathbf{i} + \Omega_2^{\mathrm{P}} \cdot \mathbf{j} + \Omega_3^{\mathrm{P}} \cdot \mathbf{k}\right) \times \left(\Omega_4^{\mathrm{P}} \cdot \mathbf{i} + \Omega_5^{\mathrm{P}} \cdot \mathbf{j} + \Omega_6^{\mathrm{P}} \cdot \mathbf{k}\right); \tag{3.22}$$

3.5 Generating virtual displacements with Hermite polynomials

The aim is to determine a polynomial function: $H(q)$, ($q \in \mathbb{R}$) defined on the interval $[q_1, q_2]$ and to satisfy the conditions:

$$\begin{array}{lll} H(q_1) = p_1; & H^{''}(q_1) = p_1^{''}; & H^{'}(q_2) = p_2^{'}; \\ H^{'}(q_1) = p_1^{'}; & H(q_2) = p_2; & H^{''}(q_2) = p_2^{''}; \end{array} \tag{3.23}$$

in which $p_{1,2}$, $p_{1,2}^{'}$, $p_{1,2}^{''}$ are respectively the values of the function of the first derivative and the second derivative at the ends of the interval.

The polynomial will therefore be of the form:

$$H(q) = a_5 q^5 + a_4 q^4 + a_3 q^3 + a_2 q^2 + a_1 q + a_0; \tag{3.24}$$

with derivatives:

$$H^{'}(q) = 5a_5 q^4 + 4a_4 q^3 + 3a_3 q^2 + 2a_2 q + a_1; \tag{3.25}$$

$$H^{''}(q) = 20a_5 q^3 + 12a_4 q^2 + 6a_3 q + 2a_2; \tag{3.26}$$

The system of equations representing the conditions (3.23) is:

$$\begin{cases} a_5q_1^5 + a_4q_1^4 + a_3q_1^3 + a_2q_1^2 + a_1q_1 + a_0 = p_1 \\ a_5q_2^5 + a_4q_2^4 + a_3q_2^3 + a_2q_2^2 + a_1q_2 + a_0 = p_2 \\ 5a_5q_1^4 + 4a_4q_1^3 + 3a_3q_1^2 + 2a_2q_1 + a_1 = p_1^{'} \\ 5a_5q_2^4 + 4a_4q_2^3 + 3a_3q_2^2 + 2a_2q_2 + a_1 = p_2^{'} \\ 20a_5q_1^3 + 12a_4q_1^2 + 6a_3q_1 + 2a_2 = p_1^{''} \\ 20a_5q_2^3 + 12a_4q_2^2 + 6a_3q_2 + 2a_2 = p_2^{''} \end{cases}; \quad (3.27)$$

The method of Hermite polynomials is based on the observation that the same conditions at the ends of the interval will be met by a polynomial function having the expression:

$$H(q) = H_1(q) + H_2(q) + H_3(q) + H_4(q) + H_5(q) + H_6(q); \quad (3.28)$$

where H_1 ... H_6 are five-degree polynomial functions.

3.5.1 Polynomial formulation of the motion parameters for the 6RSS mechanism

The motion of the characteristic point *P* in the case of the parallel mechanism 6RSS is given by the equations:

$$x = x(t);\ y = y(t);\ z = z(t); \quad (3.29)$$

The goal of this application is to determine the trajectory of the characteristic point, knowing the coordinates of the extremities of the AB and BC intervals respectively the values of the velocities and accelerations of the point *P* at the ends of the intervals. We have the points $A(-132.17, -132.17, -530)$, $B(66.58, -204.91, -415)$ and $C(-202.98, -141.64, -300)$.

A computational program was developed by means of which the coordinates of the points *P*, respectively their velocities and accelerations were determined based on given input parameters. An Excel macro has been created in order to generate the Hermite function values list.

The data obtained through the computational program was imported into a previously created AutoLisp file in which the workspace and trajectories determinated by the motion of the characteristic point of the robot was generated (Figure 3.7).

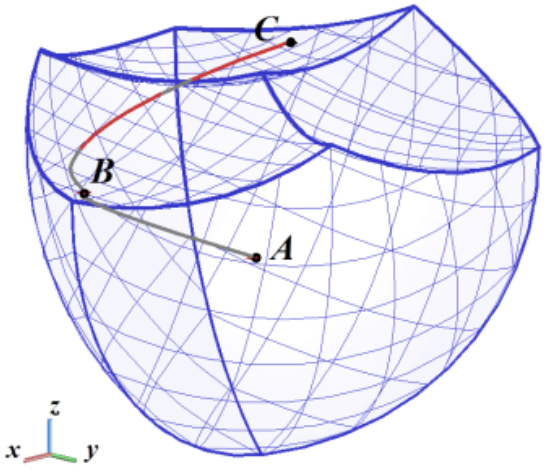

Figure 3. 7 Trajectory of point *P* through the workspace.

3.6 Determining the optimal trajectory of the characteristic point with the restriction of avoiding a given space

Based on the geometric model of the 6RSS parallel robot, the limits of the robot technological workspace were determined (Figure 3.8).

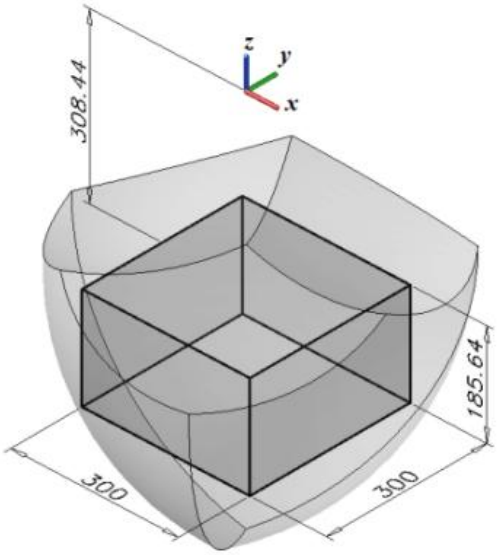

Figure 3. 8 The volume of the technological workspace.

This resulted in a rectangular parallelepiped with a square base whose volume is $V_{th} = 16.71\ \mathrm{dm}^3$.

A number of research has been carried out that highlighted the importance of the optimization process [129-135].

In the case of the problem presented, the objective function is the length of the trajectory, and the constraints are represented by the condition of avoiding a given volume within the workspace.

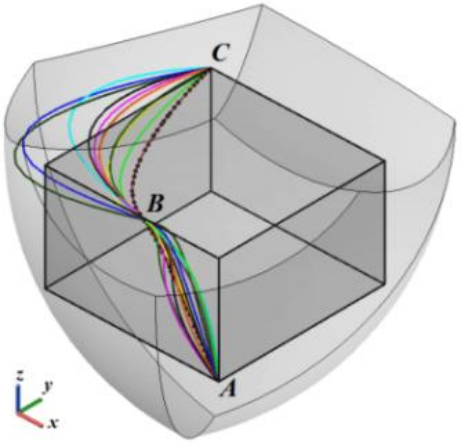

Figure 3.9 Fascicle of curves determined by the variation of the motion parameters

By varying some parameters (the displacement times from *A* to *B* or *B* to *C*, the velocity or acceleration of point *B*) we obtain a curve fascicle with different trajectories (Figure 3.9).

The optimized function in this application is the trajectory length described by the characteristic point having the expression:

$$L_c = \sum_{j=1}^{n} \left| P_{j-1} - P_j \right| \rightarrow min; \tag{3.30}$$

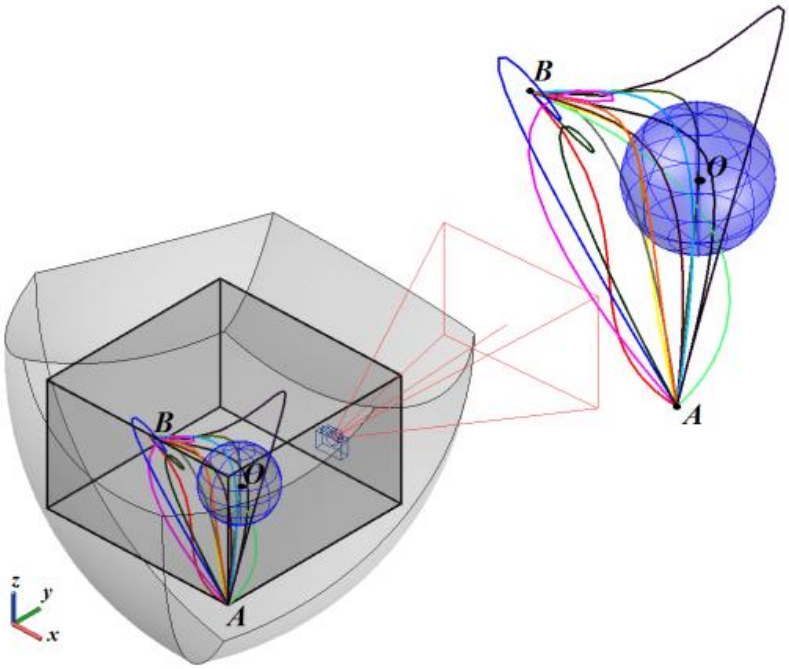

Figure 3. 10 The resulting initial trajectories.

These solutions are the initial values of the design variables. The value of the objective function is calculated with these initial values. The resulting trajectories are represented in Figure 3.10.

Thus, a series of eleven trajectories were determined of which were chosen those that satisfy the imposed conditions. Iteration continues with the same time intervals and ranges only from the velocity and acceleration of point *B*.

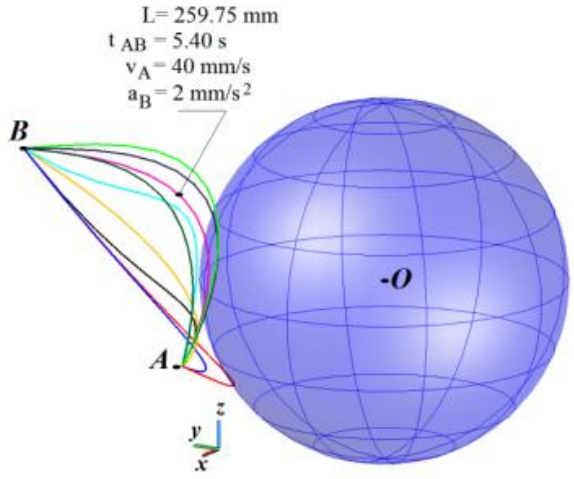

Figure 3. 11 Determination of the minimum length trajectory.

By successive calculations we determine the minimum value of the characteristic point trajectory length corresponding to an interval *j* (Figure 3.11).

3.6.1 Determining the optimal path, with the objective function minimizing its travel times

For this application, the objective function is the duration of a manipulation operation. We propose to determine an optimal trajectory of the characteristic point defined on the $h_j(\lambda)$

functions by avoiding an imposed volume inside the robot's technological workspace so that the runtime of this trajectory is minimal.

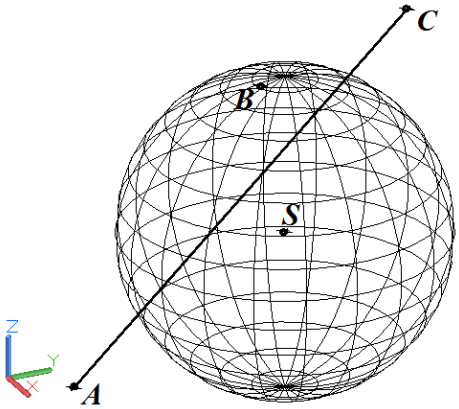

Figure 3. 12 Position of the sphere relative to the AC direction.

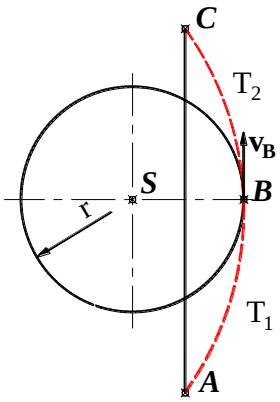

Figure 3. 13 Rotated section in spherical volume with trajectory of characteristic point.

The volume to be avoided by the end effector is the spherical surface from the inside of the robot's technological workspace. The centre of this radius $r = 80\,\text{mm}$ is $S\,(-45,\ 21, -410)$. The trajectory described by the motion of the characteristic point is analysed when the sphere is interposed on the rectilinear trajectory between the points $A(84, -150, -405)$ and $C(-130, 125, -350)$ on the ends of the interval (Figure 3.12, 3.13). In this case, the intermediate point $B(-42.64, 7.09, -331.25)$ on the trajectory described by the Hermite function belongs to the sphere so that $SB = r$ and $d(S, AC) < r$.

We consider the velocity direction in point $B, (\mathbf{v_B})$ parallel to the **AC** direction and the acceleration of point *B* equal to zero $(\mathbf{a_B} = 0)$. Thus, the three points *A, C* and *S* determine a plan ϑ containing all trajectories described by the Hermite function (Figure 3.14).

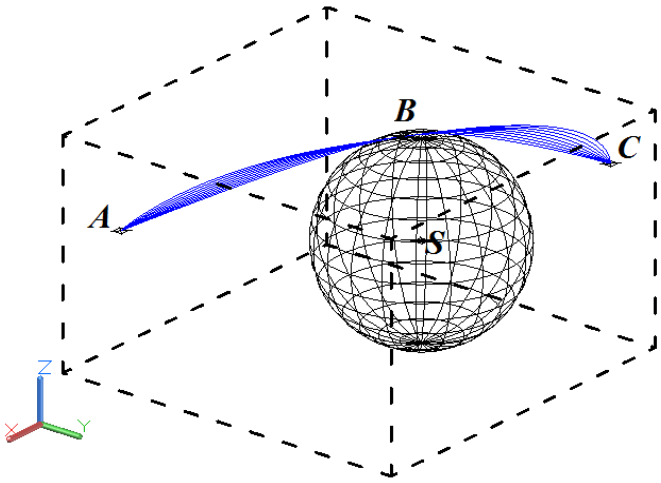

Figure 3. 14 Fascicle of curves determined by the trajectories of point *P.*

Trajectory displacement times were varied on both the AB and BC intervals between two values T_{min} and T_{max} . The optimized function for this application is the displacement time on the trajectory path described by the characteristic point. The expression of this function is:

$$T = T_{1,\text{i}} + T_{2,\text{j}} \rightarrow min; \tag{3.31}$$

3.7 Determination of singular configurations of the 6RSS parallel mechanism

Determining the singlular configurations is a central issue for the kinematic model of the robot. The issue of critical positions is subject to special studies on parallel mechanisms [136-141]. In the case of the 6RSS parallel manipulator, these singular positions can be geometrically expressed by the following two conditions:

- when point *B* belongs to the plane [P_1]determined by the unit vector **u** of the rotational joint and point *A* (Figure 3.15);
- when point *A* belongs to the plan [P_2] of the mobile platform (Figure 3.16).

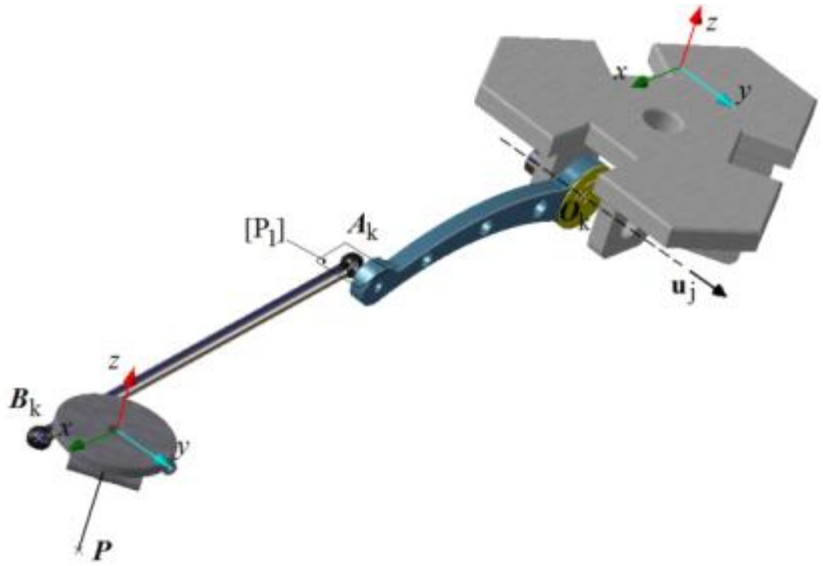

Figure 3. 15 **.** Singularity of type I, point *B* belongs to the plane [P_1].

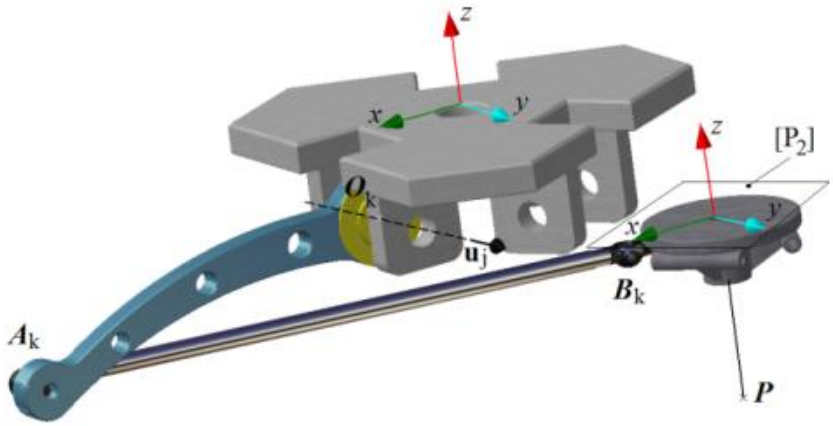

Figure 3. 16 Singularity of type II, point *A* belongs to the plane [P_2].

To determine these singular configurations, a program was created to realise three-dimensional representations of the functions of determinants $\Delta[\mathbf{B}]$ and $\Delta[\mathbf{A}]$ of the direct and inverse Jacobian matrix. Based on these three-dimensional representations, was realised sections with plans corresponding to the zero value of the two functions $\Delta[\mathbf{B}]$ and $\Delta[\mathbf{A}]$ (Figure 3.17, 3.18).

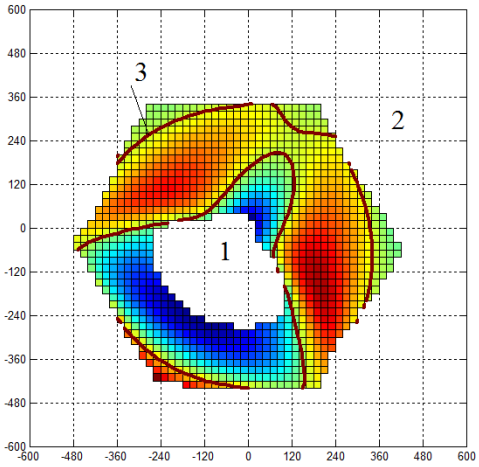

1,2 - Spaces in which the mechanism can not exist
3 - Critical curves determined by the set of singular configurations

Figure 3. 17 Section with a plane corresponding to the value $\Delta[\mathbf{A}] = 0$ for z = -200mm

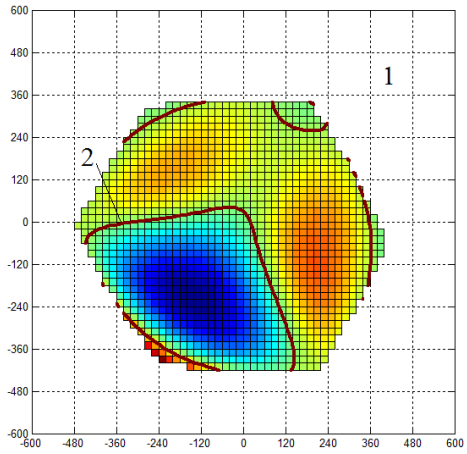

1 - Spaces in which the mechanism can not exist
2 - Critical curves determined by the set of singular configurations

Figure 3. 18 Section with a plane corresponding to the value $\Delta[\mathbf{A}] = 0$ for z = -315mm

3.8 Manipulability of parallel mechanism

The concept of manipulating robots has been introduced by Yoshikawa since 1985. He believes that when the manipulability index μ reaches the maximum, the robot is at the furthest position from a singular configuration. Manipulability for redundant robots is defined by the expression [142]:

$$\mu = \sqrt{\det([\mathbf{J}] \cdot [\mathbf{J}]^{\mathbf{T}})}; \tag{3.32}$$

in which [**J**] is the global Jacobian matrix of the robot and [**J**] **T**is transposed.

For non-redundant robots, the manipulability index μ is given by the relationship [143]:

$$\mu = |\det([\mathbf{J}])|; \tag{3.33}$$

According to some researchers, the manipulability quantifies the capacities to transmit the manipulability speed or, in other words, the robot dexterity [144]. In order to better determine manipulability, it was proposed to separate its translation and rotation movements [145].

For the kinematic quantitative evaluation of parallel robots, the manipulating ellipsoid concept was introduced. This ellipsoid is determined by the final effector speed fields **v**, which satisfies the condition:

$$|\dot{\mathbf{q}}| \leq 1; \tag{3.34}$$

This ellipsoid belongs to the robot's Euclidean *m*-dimensional space. Thus, in the direction of the major axis of the ellipsoid, the final effector will move at high speed and in the direction of the minimum axis of the ellipsoid, the end effector will travel at a low speed. If this ellipsoid is a sphere, the end effector will move uniformly in all directions.

Another dimension representative of the ellipsoid manipulability capacity is its volume. The higher the volume of the ellipsoid, the faster the end effector will move. The volume of this ellipsoid is given by the formula [146]:

$$V_{\text{eps}} = \mu \cdot c_{\text{m}}; \tag{3.35}$$

in which:

$$\mu = \sigma_1 \cdot \sigma_2 \cdot \ldots \cdot \sigma_{\text{m}}; \tag{3.36}$$

c_{m} is a constant coefficient whose expression is:

$$c_{\text{m}} = \begin{cases} \frac{(2\pi)^{\frac{m}{2}}}{2 \cdot 4 \cdot 6 \ldots \cdot (m-2) \cdot m} & \text{for } m = \text{even} \\ \frac{2 \cdot (2\pi)^{\frac{m-1}{2}}}{1 \cdot 3 \cdot 5 \ldots \cdot (m-2) \cdot m} & \text{for } m = \text{odd} \end{cases}; \tag{3.37}$$

It is known that for the matrix [**J**] of the dimension $m \times n$, $\sigma_1, \sigma_2, \ldots, \sigma_m$ represents the biggest m single values of the matrix [**J**].

3.9 Conclusions on kinematic analysis and optimization method used

Based on the kinematic analysis of the 6RSS parallel mechanism, a method for determining the optimal trajectory of the characteristic point was presented. For the purpose of defining the end efector motion, polynomial Hermite expressions of geometric parameters were used as time functions.

The polynomial variation of motion parameters was highlighted on the basis of computational programs and by means of some CAD applications the trajectory of the characteristic point within the robot workspace was determined. In the optimization process two distinct formulations of the optimization objective were addressed:

- minimizing the trajectory length of the characteristic point, belonging to the end effector element, relative to additional imposed conditions;

- minimizing the trajectory time of the characteristic point while respecting certain additional requirements imposed.

In the way of minimizing the trajectory length, elements of the classic optimization method have been highlighted based on objective functions and some restrictions.

For the second optimization, determination of the optimal solution under the given conditions was done by decomposing the trajectory into two sectors, separated by an imposed point of it. The optimization problem was solved by a numerical analysis of the parameters.

Cap. 4 Dynamic analysis of the 6RSS parallel mechanism

4.1 Aspects of the dynamic analysis of the parallel mechanisms

Based on the classical theory of mechanical dynamics, numerous research has been carried out on the dynamic performance of various parallel mechanisms [147-167].

Several methods of dynamic analysis of parallel mechanisms have been identified among which the most commonly used approach is based on the Newton-Euler formula of the d'Alembert principle. Through this method, the Newton-Euler equations are applied to each body isolated from the rest of the mechanism. Using this method, all the forces $\Sigma\sum \mathbf{F}_{\mathrm{jk}}$ and the connecting moments $\sum \mathbf{M}_{\mathrm{jk}}$ from each kinematic coupling A_{jk} obtained from the O_{jk} origin of the local coordinate system attached to each body $\mathcal{C}_{\mathrm{jk}}$ (Figure 4.1) are obtained.

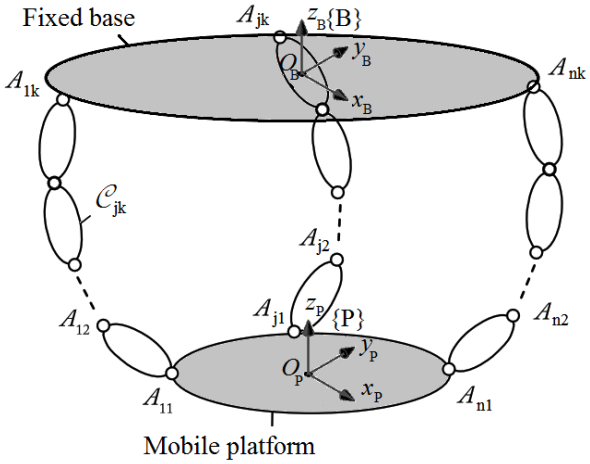

Figure 4.1 General representation of the parallel mechanism.

We point out that $\sum \mathbf{F}_{\mathrm{jk}}$ is the resultant of the external forces $\mathbf{R}_P$, acting at the point *P*, and $\sum \mathbf{M}_{\mathrm{jk}}$ is the resultant moment $\mathbf{M}_G$, of the external forces applied to the platform in the center of gravity G.

Forces and moments of inertia have the expressions:

$$\mathbf{R}_P = \sum \mathbf{F}_{\mathrm{jk}} = m_{\mathrm{jk}}\,\dot{\mathbf{v}}_{\mathrm{jk}} + \dot{\boldsymbol{\omega}}_{\mathrm{jk}} \times \mathbf{M}_{\mathbf{S}_{\mathrm{jk}}} + \boldsymbol{\omega}_{\mathrm{jk}} \times \left(\boldsymbol{\omega}_{\mathrm{jk}} \times \mathbf{M}_{\mathbf{S}_{\mathrm{jk}}}\right); \tag{4.1}$$

$$\mathbf{M}_G = \sum \mathbf{M}_{\mathrm{jk}} = \mathbf{I}_{O_{\mathrm{jk}}}\,\dot{\boldsymbol{\omega}}_{\mathrm{jk}} + \mathbf{M}_{\mathbf{S}_{\mathrm{jk}}} \times \dot{\mathbf{v}}_{\mathrm{jk}} + \boldsymbol{\omega}_{\mathrm{jk}} \times \left(\mathbf{I}_{O_{\mathrm{jk}}}\,\boldsymbol{\omega}_{\mathrm{jk}}\right); \tag{4.2}$$

Another approach for determining the dynamic model is based on Lagrange equations that use kinetic and potential energy expressions [168, 169]. This model is expressed synthetically through the system of differential equations [170]:

$$\frac{\mathrm{d}}{\mathrm{dt}}\left(\frac{\partial \mathrm{E}}{\partial \dot{\mathbf{q}}}\right) - \frac{\partial \mathrm{E}}{\partial \mathbf{q}} + \frac{\partial \mathrm{U}}{\partial \mathbf{q}} = \boldsymbol{\tau} - \mathbf{J}^{\mathrm{T}}(\mathbf{q}, \mathrm{t})\boldsymbol{\lambda}; \tag{4.4}$$

Lagrange equations lead to a dynamically expressed model based on the relationship [171]:

$$\boldsymbol{\tau} = \mathbf{M}(\mathbf{q})\ddot{\mathbf{q}} + \mathbf{c}(\mathbf{q}, \dot{\mathbf{q}}); \tag{4.5}$$

De Another way to dynamically analyze parallel mechanisms is based on the principle of virtual mechanical work, which determines the forces of inertia and the moments acting on the mobile platform and the actuating arms [172-174]. This dynamical model is based on d 'Alambert's principle that the power $\mathbf{P_I}$ resulting from the forcing forces of a body moving at a virtual (linear and / or angular) speed $\mathbf{v}_{virt}$ respectively $\boldsymbol{\omega}_{virt}$ is equal to the sum of the power

$\mathbf{P}_{\mathbf{F_{ext}}}$ resulting from the external forces applied to the body and the power $\mathbf{P}_{\mathbf{F_{int}}}$ resulting from the internal forces applied to it (4.6).

$$\mathbf{P_I} = \mathbf{P}_{\mathbf{F_{ext}}} + \mathbf{P}_{\mathbf{F_{int}}}; \tag{4.6}$$

4.2 Dynamic model of the 6 RSS parallel mechanism based on the d 'Alembert's principle

The dynamic model, like the other models used in the study of the mechanisms, has two complementary practical formulations: the dynamic dynamic model and the inverse dynamic pattern.

In the case of the dynamic model, actuator $\mathbf{M}_a$ torques and inertial characteristics are known and the trajectory, velocity and acceleration of the characteristic point are determined. In the case of the reverse dynamic model, the trajectory, velocity and acceleration of the characteristic point of the end effector is known, and the actuator torques $\mathbf{M}_a$ of the actuating joints are determined.

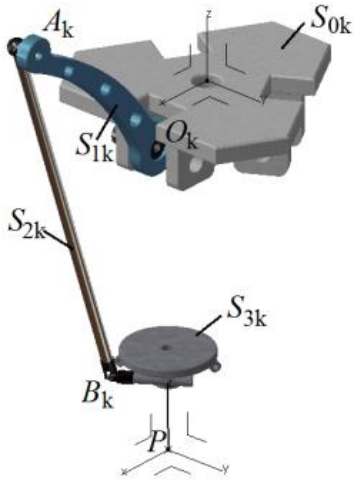

Figure 4. 2 Representing one of the kinematic *k* chains of the 6RSS parallel mechanism.

The system of equations (4.7) containing the equations of dynamic equilibrium of the D'Alembert for each isolated element S_{jk} of the mechanism.

$$\begin{cases} \sum \mathbf{R} = 0 \\ \sum \mathbf{M} = 0 \end{cases}; \tag{4.7}$$

The two sums of forces and moments from relation (4.7) have the expression:

$$\sum \mathbf{R} = \mathbf{R}_{\mathbf{I}_j} + \mathbf{R}_{\mathbf{L}_j} + \mathbf{R}_{\mathbf{A}_j} = 0; \tag{4.8}$$

$$\sum \mathbf{M} = \mathbf{M}_{\mathbf{R}_{\mathbf{I}_j}} + \mathbf{M}_{\mathbf{R}_{\mathbf{L}_j}} + \mathbf{M}_{\mathbf{R}_{\mathbf{A}_j}} = 0; \tag{4.9}$$

The calculation algorithm involves the following steps:

1. Each mobile element S_{jk} of the mechanism is sequentially isolated and is represented: applied forces, reactions forces. the torsion elements of the inertial forces reduced to the center of gravity.
2. The cinematic equilibrium equations for each body are written, finally obtained the *6n* equations for *n* number of elements;
3. Relationships between body accelerations are established;

4. It solves the system of algebraic equations containing the kinetostatic equilibrium equations, resulting the reactions of the joints (forces and moments).

The principle of d 'Alembert was applied to one of the six kinematic *k* chains of the mechanism. We isolate the mobile element S_{11} and write the kinetostatic equilibrium equations for this body (Figure 4.3).

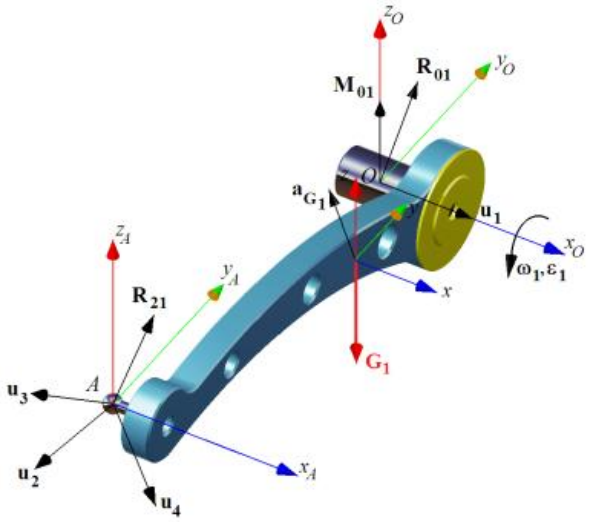

Figure 4. 3 Applying the principle of d'Alembert for the mobile element S_{11}.

We write the D'Alembert equations of dynamic equilibrium corresponding for the element S_{11} (Figure 4.3):

$$\begin{cases} \mathbf{R_{I_1}} + \mathbf{R_{L_1}} + \mathbf{R_{A_1}} = 0 \\ \mathbf{M_{R_{I_1}}} + \mathbf{M_{R_{L_1}}} + \mathbf{M_{R_{A_1}}} + \mathbf{M_{01}} = 0 \end{cases}; \tag{4.16}$$

Similarly, we apply the same principle to body S_{21}, (Figure 4.4), and write the kinetostatic equilibrium equations for it:

$$\begin{cases} \mathbf{R_{I_2}} + \mathbf{R_{L_2}} + \mathbf{R_{A_2}} = 0 \\ \mathbf{M_{R_{I_2}}} + \mathbf{M_{R_{L_2}}} + \mathbf{M_{R_{A_2}}} + \mathbf{M_{32}} = 0 \end{cases}; \tag{4.17}$$

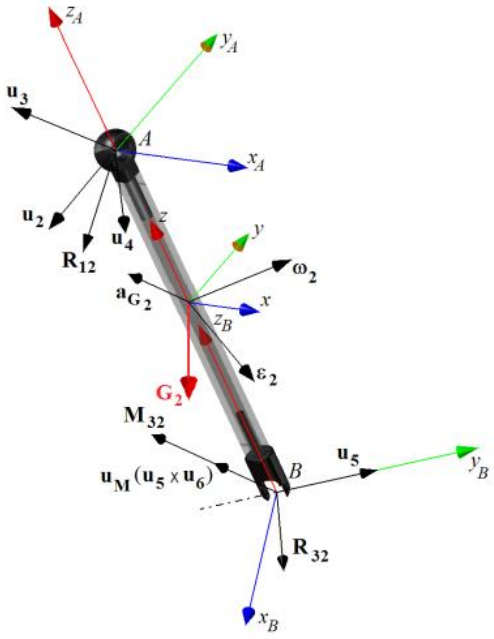

Figure 4. 4 Applying the principle of d'Alembert for the mobile element S_{21}.

Finally, we apply the same principle to body S_{31}, (Figure 4.5), and write the kinetostatic equilibrium equations for it:

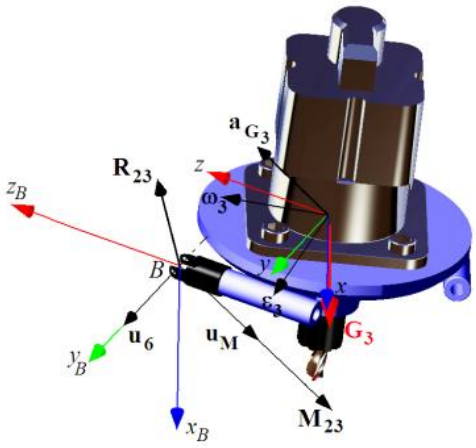

Figure 4.5 Applying the principle of d'Alembert for the mobile element S_{31}.

$$\begin{cases} \mathbf{R}_{\mathbf{I}_3} + \mathbf{R}_{\mathbf{L}_3} + \mathbf{R}_{\mathbf{A}_3} = 0 \\ \mathbf{M}_{\mathbf{R}_{\mathbf{I}_3}} + \mathbf{M}_{\mathbf{R}_{\mathbf{L}_3}} + \mathbf{M}_{\mathbf{R}_{\mathbf{A}_3}} + \mathbf{M}_{\mathbf{23}} = 0 \end{cases}; \tag{4.18}$$

Given that for the thirteen mobile elements of the 6RSS parallel mechanism are written six equivalent equations of equilibrium, we will produce seventy-eight equations plus six equations of orthogonality having the form $\mathbf{M_{0k}} \cdot \mathbf{u_k} = 0$, in a total of eighty-for equations. By resolving these equations will result forces and moments of kinematic joints.

4.3 Analysis of power losses in spherical joint

The importance of spherical joints has led many researchers to developed a series of studies to determine their influence on the dynamics of mechanical systems [175-183].

In this subchapter there is presented a method for determining the power lost by the 6RSS parallel mechanism by friction between the components of the spherical joints that make up the six kinematic chains thereof. Determination of these power losses in the spherical joints was done in an application where the characteristic point it's moving on a closed space curve, neglecting the inertial forces, the movement being performed very slowly.

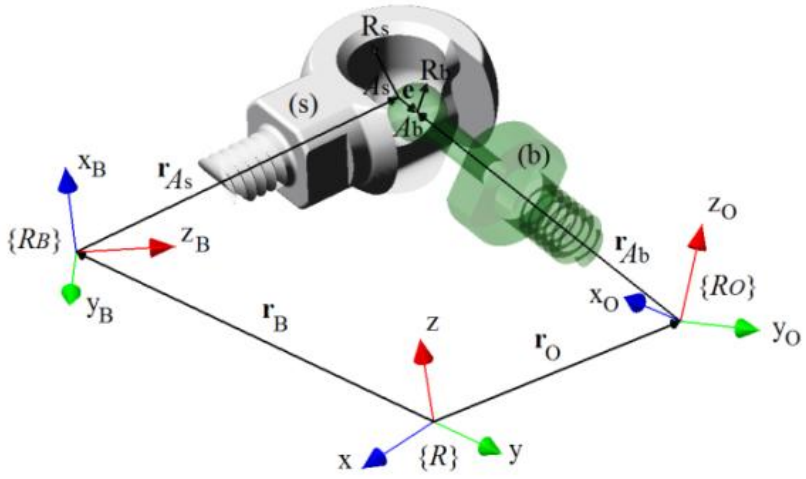

Figure 4.6 Representing spherical joint with point position A_s and A_b.

Using the Catia software, the variation graphs of the versor $\mathbf{u_2}$ of the direction **AB** and of the vector $\boldsymbol{\omega}_{21}$ have been determined depending on the position of the point P_j on the given spatial

curve. The trajectory of a point belonging to the spherical head of the spherical kinematic joint of the parallel mechanism was obtained and the graphs of the traiectory's projections on the three plans XY, ZX, YZ were done.

Figure 4.6 shows the spherical joint of one of the A_{k} points.

It has been done an application in which was considered the characteristic point *P* in motion on a spatial curve of length $\mathrm{L} = 528.637\ \mathrm{mm}$, when $\beta \neq \gamma \neq 0 = ct$ and α is variable (α, β, γ are the three orientation parameters of the mobile platform). In this application, the point *P* is in permanent contact with the curve. It has been stated that in the application done through the Catia software, the motion parameter is an arc of curve by equal length, dividing the curve into 72 equally distributed points on it, whose Cartesian coordinates are returned by the program.

The particularity of the application is that the inertia forces $\mathbf{F_i}$ are neglected, the motion being performed very slowly, therefore, there is only one axial force $\mathbf{F_{21}}$ acting in the **AB** direction (Figure 4.7).

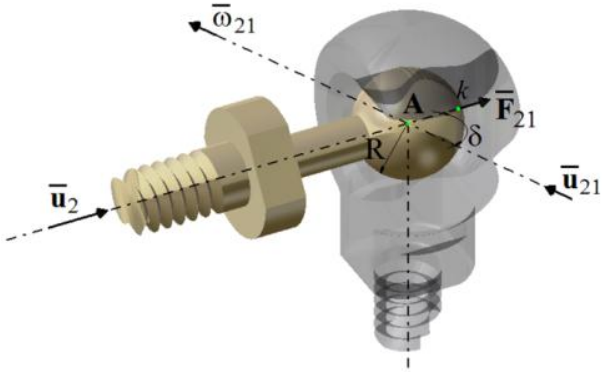

Figure 4. 7 Highlighting the point of contact k of the spherical joint *A*.

It has been noted with δ the angle between versor $\mathbf{u_2}$ and the versor $\mathbf{u_{21}}$ and with R the radius of the spherical head of the joint. Also $\boldsymbol{\omega}_{\mathbf{21}}$ is the angular velocity of the contact point k. Taking into account the imposed condition $\mathbf{F_i} = 0$, it can be written the following expression for the power loss $\mathbf{P_f}$ determinated by friction between the kinematic joint elements in point *A*:

$$\mathbf{P_f} = \mu \cdot \mathbf{F_{21}} \cdot \boldsymbol{\omega}_{\mathbf{21}} \cdot \mathrm{R} \cdot \sin\delta; \tag{4.19}$$

The mechanical work of friction forces is:

$$\mathbf{L_f} = \int_0^T \mathbf{P_f}\, dt = \mu \cdot \mathbf{F_{21}} \cdot \mathrm{R} \int_0^{\mathrm{T}} (\boldsymbol{\omega}_{\mathbf{21}} \cdot \sin\delta)\, dt; \tag{4.20}$$

The integration of formula (4.20) was done numerically with the trapeze method, using the finite formula:

$$\mathbf{L_f} \approx \mu \cdot \mathbf{F_{21}} \cdot \mathrm{R} \sum_{\mathrm{i}=1}^{72} (\boldsymbol{\omega}_{\mathbf{21}} \cdot \sin\delta)_{\mathrm{i}} \cdot \Delta\mathrm{t}\,; \tag{4.21}$$

where:

$$\Delta\mathrm{t} = \frac{T}{72}\,[s]; \tag{4.22}$$

represents the time required to go through one of the 72 equal circle arcs.

Admitting a constant speed of motion of the point on the curve, $v = 10\ \mathrm{mm/s}$, and knowing its length (L), results the time T required for following the curve:

$$T = \frac{L}{v} = 52.8637\ s \rightarrow \Delta\mathrm{t} = 0.7342\ [s]; \tag{4.23}$$

By admitting a friction coefficient $\mu = 0.2$, it can be determined the lost power by friction $\mathbf{P_f}$ in the kinematic joint of point *A* for each position P_{j} of the characteristic point. By summing these values, it has been obtained the frictional power losses in the *A* kinematic joint:

$$\mathbf{P_f} = \mu \cdot R \sum_{i=1}^{72} (\boldsymbol{\omega_{21}} \cdot \sin\delta)_i = 0.13 \text{ [W]}; \quad (4.24)$$

Using the above application, with the displacement of the characteristic point on the space curve, we will further determine the trajectory of the contact point k from a spherical joint A_k taking into account the effect of the inertial forces.

By varying the load on one of the spherical joints A_k of the parallel mechanism, we obtain different trajectories of the contact point k. As can be seen from Figure. 4. 8 the length of these trajectories is directly proportional with the load of the joint.

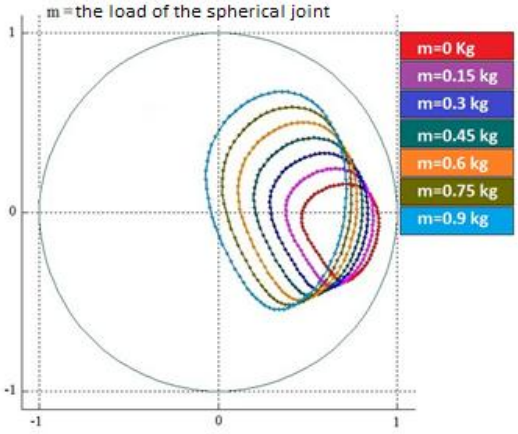

Fig. 4.8 Modify the described trajectories by point k depending on the load in the joint

Cap. 5 General conclusions, original contributions and perspectives

5.1 General conclusions

The scientific research and scientific work undertaken during the three years of doctoral studies on parallel mechanisms in general and parallel mechanisms with six degrees of freedom in particular, allowed the synthesis of scientific results and the highlighting of their main aspects required in the design and control process.

The main aspects studied and described in the Ph.D. thesis concern the analysis of the working space, the kinematics and the dynamics of a new complex parallel mechanism with six degrees of freedom with a configuration that allows its applicability in various fields.

Determining the geometric model (imposed by the structural particularities of the 6RSS parallel mechanism) is a necessary step in the exploitation of the robot. The motion of the platform is defined by an overlap of two motion: a translation one given by the displacement of the characteristic point and a spherical rotation determined by the change of its orientation relative to the one fixed reference system.

The multitude of the mobile platform positions were separated into two three-dimensional spaces that allow a more rigorous analysis of the geometric properties of the parallel mechanism, but also a representation closer to the human perception of the two spaces.

A method has been developed to determine the workspace of the robot that can be extrapolated and to model other structural schemes. For this purpose, computational algorithms and software applications were created to determine the optimum workspace of the 6 RSS parallel mechanism. These applications offer the opportunity to optimize this workspace for the efficient exploitation of the parallel mechanism under review. Determining the dimensions of the technological space as accurately as possible determines the limits between which kinematic parameter values can be controlled.Pentru definirea mișcărilor elementului efector au fost utilizate expresii polinomiale Hermite ale parametrilor geometrici ca funcții de timp.

For the purpose of defining the displacement of the end efector element, polynomial Hermite expressions of geometric parameters were used as time functions.

Various methods have been presented for determining the angular speeds of the actuators of the parallel mechanism. The described applications are different ways of approaching the robot's kinematic problem.

Based on some computational programs, the polynomial variation of the motion parameters was highlighted, and with the help of some CAD applications, the trajectory of the characteristic point within the robot workspace was determined. The angular speeds of the actuating arms could also be determined when the end effector follows the trajectory described by the Hermite function.

The optimization process was aimed at:

- minimizing the trajectory length of the characteristic point, belonging to the effector element, subject to additional imposed conditions;
- minimizing the trajectory time of the characteristic point while respecting certain additional imposed conditions.

The optimization problem was solved by a numerical analysis of the parameters. This way of solving the optimization problem was chosen to avoid an analytical formulation of the objective function.

Based on the two Jacobian matrices, the two types of singularities encountered in the parallel mechanisms were defined, realising three-dimensional representations of the functions of the determinants of the two matrices. With the help of the same program, there were sections that highlight critical curves for a given position and orientation.

To determine the dynamic model, an application was made to force the movement of the characteristic point inside the robot technological space between two extreme positions A and C on a trajectory whose curve is determined by an intermediate point B located thereon.

The dynamic modeling of the parallel mechanism was done using the kinetostatic method based on d'Alembert's principle.

Determination of the inertial characteristics of the moving elements belonging to the analyzed mechanism was done by means of a CAD softwere for the imposed movement.

For each of the six kinematic k chains of the mechanism, seventy-eighth of equations plus six orthogonality equations in total eighty-two equations resulted. By solving them the forces and moments of the kinematic joint were determined.

The study of the loss of power in spherical joints was done on a concrete case, based on the kinematic and dynamic analysis of the 6RSS parallel mechanism.

The trajectories described by the contact point were analyzed in two different cases:

- in the first case the forces of inertia were neglected, the movement being carried out at very low speed;
- in the second case the analysis was done based on the dynamic model, varying the load in the spherical joint

Based on the original programs, were highlighted the trajectory of the contact point belonging to the spherical joint.

Chapter 5 presents the conclusions of the entire research work and highlights personal contributions in the field of geometrical, kinematic and dynamic modeling of parallel mechanisms.

5.2 Personal contributions

Achieving the research objectives proposed for this work were based on the following original personal contributions:

• Doing up-to-date documentation on parallel mechanisms and highlighting the main aspects of them needed in the design and control process;

• Developing a method for determining the technological workspace of the robot that can be extrapolated and for modeling other structural schemes;

• Creating computational algorithms and software applications through which the optimal workspace of the parallel manipulator could be determined;

• Creating original AutoLISP codes to determine the tangible space of the robot;

• Achievement of computational programs which revealed the polynomial variation of the movement parameters;

• Creation of original AutoLISP codes that allowed the realization of three-dimensional representations of the determinant functions of the two Jacobian matrices;

• Creating computational algorithms that have solved the dynamic problem;

• Development of an original method for determining the power losses due to friction between the components of the spherical joints of the parallel mechanism.

5.3 Research perspectives

• Realization of an experimental stand with the 6RSS parallel mechanism and the study of its real behaviour

• Deepening research to find new, more effective methods for kinematic and dynamic analysis of parallel mechanisms;

• Expanding research into other types of parallel mechanisms;

• Creating programs to optimize the trajectory based on PSO algorithms.

List of published and presented works

A. Article published in ISI indexed publication

[1] Milica, L., Năstase, A., Andrei, G.: A new insight into the geometric models and workspace volume of the 6 RSS manipulator by disjunction of the translational and orientation subspaces, Mech. and Mach. Theory, vol. **121**, 804–828, doi.org/10.1016/j.mechmachtheory/201712.004.

[2] Milica, L., Năstase, A., Andrei, G.: Optimal path planning for a new type of 6RSS parallel robot based on virtual displacements expressed through Hermite polynomials, Mech. and Mach. Theory, vol. **126,** 14–33, doi.org/10.1016/j.mechmachtheory.2018.03.015, (Impact Factor: **2.577**).

B. Article published in the volume of an ISI Proceedings indexed scientific manifestation

[3] Milica, L., Andrei, G.: Particularities of fully-parallel manipulators in 6-DOFs robots design: a review of critical aspects, MATEC Web of Conferences, vol. **94**, (2017), doi.org/10.1051/matecconf/20179405003.

[4] Milica, L., Andrei, G.: Inference of power loss in spherical joints of the 6RSS parallel mechanism, MATEC Web of Conferences, vol. **137**, (2017), doi.org/ 10.1051/ matecconf/201713704002.

C. Articles published in the volumes of international conferences

[5] Milica, L., Năstase, A., Andrei, G.: Determining workspace parameters for a new type of 6RSS parallel manipulator based on structural and geometric models, MATEC Web of Conferences, vol. **112**, (2017), doi.org/10.1051/ matecconf/201711205010.

D. Articles presented at international conferences

[6] Milica, L., Andrei, G.: The calculation of the power losses from the spherical joints for the 6RSS parallel mechanism, The 5th Scientific Conference of Doctoral Schools of UDJG, Galati, 2017, România.

[7] Milica, L., Amorțilă, V., Andrei, G.: Models of kinematic analysis applied to complex parallel mechanisms, The 6th Scientific Conference of Doctoral Schools of UDJG, Galati, 2018, România.

[8] Milica, L., Năstase, A., Andrei, G.: Kinematic analysis of a new 6RSS parallel manipulator performing a certain working operation, The 8th International Conference on Advanced Concepts in Mechanical Engineering, Iași, 2018, România.

References

[1] J. P. Merlet, *Parallel robots. 2nd ed*., (2006).
[2] D. Zhang, *Parallel robotic machine tools*, (2010).
[3] J. P. Merlet, Tehnical Report 1645, INRIA, (1992).
[4] C. Gosselin, J. Angeles, J. Mech. Transm.-T. ASME., **110**, 35-41, (1988).
[5] J. Gallardo, R. Rodrıguez, M. Caudillo, J. M. Rico, Mech. Mach. Theory, **43**, 201–216, (2008).
[6] R. Di Gregorio, J. Mech. Transm.-T. ASME., **126**, 850–855, (2004).
[7] C. M. Gosselin, J. Angeles, J. Mech. Transm.-T ASME., **111**, 202–207, (1989).
[8] Y. Zhang, C. Crane, J. Duffy, J. Robotic Syst., **15**, 299–308, (1998).
[9] K. Wohlhart, Mech. Mach. Theory, **29**, 581–589, (1994).
[10] C. Innocenti, V. Parenti-Castelli, Mech. Mach. Theory, **28**, 553–561, (1993).
[11] K. M. Lee, D.K. Sha, *Proceedings IEEE/ICRA*., **1**, 345–350, (1987).
[12] H. S. Kim, L.W. Tsai, J. Mech. Transm.-T. ASME., **125**, 92–97, (2003).
[13] C. H. Liu, S. Cheng, J. Mech. Des. ASME., **126**,1006–1016, (2004).
[14] Z. Huang, Y. Fang, Mech. Mach. Theory, **31**, 1009–1018, (1996).
[15] Y. Fang, Z. Huang, Mech. Mach. Theory, **32**, 789–796, (1997).
[16] Z. Huang, J. Wang, Mech. Mach. Theory, **36**, 893–911, (2001).
[17] S. K. Agrawal, *Proceedings of 8th World Congress on TMM*, 405-408, (1990).
[18] Z. Huang, J. Wang, *Proceedings of A Symposium Commemorating of Sir Robert Stawell Ball*, (2000).
[19] Z. Huang, J. Wang, Y. Fang, Mech. Mach. Theory, **37**, 229–240, (2002).
[20] J. Merlet, C. Gosselin, N. Mouly, Mech. Mach. Theory, **33**, 7-20, (1998).
[21] F. Bulca, J. Angeles, P.J. Zsombor-Murray, Mech. Mach. Theory, **34**, 497-512, (1999).
[22] A. Kosinska, M. Galicki, K. Kedzior, J. Robotic Syst., **20**, 539-548, (2003).
[23] M. Arsenault, R. Boudreau, J. Robotic Syst., **21**, 259-274, (2004).
[24] E., Ottaviano, M.,Ceccarelli: Optimal design of CAPAMAN with prescribed workspace, Computational Kinematics, 35–44, (2001).
[25] D., Zhang: Parallel robotic machine tools. (New York), (2010).
[26] A.,Khoukhi, L.,Baron, M.,Balazinski,: Rob. Comput. Integr. Manuf., **28**: 756–769, (2009).
[27] S., Sen, B., Dasgupta, A.,K., Mallik,: Mech. Mach. Theory, **38**: 1165–1183, (2003).
[28] M., Arsenault, and R., Boudreau: J. Robotic Syst, **21**: 259-274, (2004).
[29] J., Gallardo, R., Rodrıguez, M., Caudillo, J.,M., Rico: Mech. Mach. Theory, **43**: 201–216 (2008).
[30] A., Stoica, D., Pisla, S., Andras, B.,Gherman, B.,Z., Gyurka, N., Plitea,: Mech. Eng., **8**: 70–79, (2013).
[31] P.,C., Lee, J.,J., Lee: Mech. Eng., **7**: 163–187, (2012).
[32] I.,A., Bonev, J., Ryu: Mech. Mach. Theory, **36**: 1-13, (2001).
[33] A. Dunning, G. Tolou, Int. J. Mech. Sc., **2**, 157–168, (2011).
[34] L.-W. Tsai, *Robot Analysis:The Mechanics of Serial and Parallel Manipulator*, (1999)
[35] D. Chablat, P. Wenger, IEEE Trans. Robot. Autom., **19**, 403–410, (2003)
[36] X. J. Liu, J. Wang, F. Gao, L.P. Wang, IEEE Trans. Robot. Autom., **17**, 959–968, (2001).
[37] C. Reboulet, R. Pigeyre, *Proceedings of the ISRAM.*, 293–298 (1990).
[38] M. Valenti, ASME. Mech. Eng., **17**, 70–75, (1995).

[39] K. Cleary, T. Brooks, *Proceedings of the IEEE/ICRA.*, 708–713 (1993).
[40] Z. Zhou, J. Xi, J. Mech. Des. **128**, 403–412, (2006).
[41] D. Hong et al*,* Mech. Struct. Mach., **31**, 509–528, (2003).
[42] J. Angeles, Springer, (1997).
[43] V. Parenti-Castelli, R. Di Gregorio,.J. Mech. Des., **122**, 294–298, (2000).
[44] D. Stewart*. Proceedings of Int.Mech.Eng*., **15**, 371–386, (1965).
[45] R. Clavel, *Proceedings of the ISR.,* (1988).
[46] S. Staicu, D.C. Carp-Ciocardia, *Proceedings of the IEEE/ICRA.*, 416–412, (2003).
[47] L.W. Tsai, R. Stamper, ASME. Des. Eng. Tech. Conf., (1996).
[48] J. M. Hervé, F. Sparacino*, Proceedings of the ARK.*, (1992).
[49] G. Gogu, *Report ROBEA MAX CNRS*, (2003).
[50] T. G. Ionescu, Mech. Mach. Theory, **38**, (2003).
[51] G. Gogu, Mech. Mach. Theory, **40,** 1068–1097, (2005).
[52] C. Gosselin, J. Angeles, J. Mech. Transm.-T. ASME., **111**, 202–207, (1989).
[53] B. Dasgupta, T.S. Mruthyunjaya*,* Mech. Mach. Theory, **34**, 1135–1152, (1998).
[54] L.W. Tsai, *Robot Analysis: The Mechanics of Serial and Parallel Manipulator*, (1999).
[55] T.R. Kane, D.A. Levinson, *Dynamics, Theory and Applications,* (1985).
[56] M. Sorli, C. Ferarresi, M. Kolarski, B. Borovac, M. Vucobratovic, Mech. Mach. Theory, **32**, 51–77, (1997).
[57] Z. Geng, L.S. Haynes, J.D. Lee, R.L. Carroll, Robot. Autonom. Syst., **9**, 237–254 (1992).
[58] L.W. Tsai, R. Stamper, ASME. Des. Eng. Tech. Conf., (1996).
[59] A.V. Nguyen, B.C. Bouzgarrou, K. Charlet, A. Béakou, Mech. Mach. Theory, **93**, 65–82 (2015).
[60] S. Staicu, X.J. Liu, J. Li, Springer, **58**, 217–235, (2009).
[61] B. Dasgupta, T.S. Mruthyunjaya, Mech. Mach. Theory, **33**, 711–725, (1998).
[62] C.L. Lin, H.Y. Jan, J.R. Lin, T.S. Hwang, Eur. J. Control, **3**, 201–212, (2008).
[63] S. Parsa, R. Boudreau, J.A. Carretero*,* Mech. Mach. Theory, **85**, 53–63, (2015).
[64] P.C. Lee, J.J. Lee, Mech. Eng., **7**, 163–187, (2012).
[65] K.H. Hunt, Cambridge University Press, (1978).
[66] J. P. Merlet, Int. J. Robot. Res., **8**, 45–56, (1989).
[67] C. Gosselin, J. Angeles, *Proceedings of IEEE T. Robotic. Autom*., **6**, 281–290, (1990).
[68] J. Craig, *Introduction to Robotics, Mechanics and Control*, *Third Edition*, (2005).
[69] D. Zlatanov, I.A. Bonev, C. Gosselin, *Proceedings of the IEEE/ICRA,* 496–502, (2002).
[70] A. Wolf, M. Shoham, J. Mech. Transm.-T. ASME., **125**, 564–572, (2003).
[71] R. Penne, E. Smet, P. Klosiewicz, J. Intell. Robot. Syst., **62**, 205–216, (2011).
[72] S. Staicu. Robotica, **27**, 199–207, (2009).
[73] F. Hao, J.M. McCarthy, J. Robot. Syst. **15**, 43–55 (1998).
[74] A. Dandurand, *The rigidity of compound spatial grids*., **10**, 41–56, (1984).
[75] A. Stoica, D. Pisla, S. Andras, B. Gherman, B.Z. Gyurka, N. Plitea, Mech. Eng., **8** ,70–79, (2013).
[76] C. Gosselin, J. Angeles, IEEE T. Robotic. Autom., **6**, 281–290, (1990).
[77] O. Ma, J. Angeles, *Proceedings of the IEEE ICRA.*, 1542–1547, (1991).
[78] B.P Horin, S. Moshe, Mech. Mach. Theory, **41**, 958–970, (2006).
[79] Z. Tong, J.F He, H.Z. Jiang et al, Robotica, **30**, 305–314, (2012).
[80] A. Hara, K. Sugimoto, J. Mech. Transm.-T. ASME.,**111**, 34–39, (1989).
[81] M. Taniguchi, M. Ikrda, A. Inagaki*,* Int. J. Jpn. Soc. Precis. Eng., **26**, 35–40, (1992).
[82] Y. Yun, Y. Li, Springer, **61**, 829–845, (2010).

[83] J. Wang, C. Gosselin, J. Mech. Transm.-T. ASME., **126**, 109–118, (2004).
[84] I. Ebrahimi, J.A. Carretero, R. Boudreau, Mech. Mach. Theory, **42**, 1007–1016, (2007).
[85] S. Lee, S. Kim, *Proceedings of the IEEE/CDC.*, **2**, 1097–1102, (1993).
[86] R. Boudreau, S. Nokleby, Mech. Mach. Theory, **56**, 138–155, (2012).
[87] K.E. Zanganeh, J. Angeles, *Proceedings of IEEE/ICRA*., 3043–3048, (1994).
[88] H. Cheng, G.F. Liu, Y.K. Yiu, Z.H. Xiong, Z. Li, *Proceedings of the IEEE/IROS*, 171–176, (2011).
[89] J. P. Merlet, *Redundant parallel manipulators*, **8**, 17–24, (1996).
[90] J. Wang, C. Gosselin, J. Mech. Des., **126**, 109–118, (2004).
[91] J. Kotlarski, B. Heimann, T. Ortmaier, Mech. Eng., **7**, 120–134, (2012).
[92] P. Last, C. Budde, J. Hesselbach,. *Proceedings of the 2005 IEEE/CASE.*, 393–398, (2005).
[93] Y. Jin, I.M. Chen, G.L. Yang, Mech. Mach. Theory, **44**, 912–922, (2009).
[94] E. Ottaviano, M. Ceccarelli*, Optimal design of CAPAMAN with prescribed workspace*, 35–44, (2001).
[95] D.I. Kim, W.K. Chung, Y. Youm, IEEE/ICRA., 2986-2991, (1997).
[96] I.A. Bonev, J. Ryu, Mech. Mach. Theory, **36**, 15-28, (2001).
[97] A. Năstase, *Mecanica Roboţilor*, **2**, 24-30, (2012).
[98] J.P. Merlet, Mech. Mach. Theory, **29**, 1099-1113, (1994).
[99] I.A. Bonev, J. Ryu*,* Mech. Mach. Theory, **36**, 1-13, (2001).
[100] Y. Lu, X. Li, C. Zhang, Y. Liu, Robotica, 1-16, (2014).
[101] H. Lim, S.H. Lee, B.R. So, B.J. Yi, Int. J. Cont. Autom. and Syst., **13**, 942-950, (2015).
[102] M. Majid, Z.A. Huang, Y.L. Yao, Int. J. Adv. Manuf. Tech., **16**, 441–449, (2000).
[103] G. Coppola, D. Zhanga, K. Li, Robot. Cim.-Int. Manuf., **30**, 99–106, (2014).
[104] K. Arrouk, B. Bouzgarrou, G. Gogu, Appl. Mech. Mater., **162**, 131-140, (2012).
[105] K. Arrouk, B. Bouzgarrou, G. Gogu, RAAD., (2010).
[106] K. Arrouk, B. Bouzgarrou, G. Gogu, Springer, **5**, 605-612, (2010).
[107] I.A. Bonev, Analysis and design of 6-dof 6-PRRS parallel manipulators, 32-33, (1998).
[108] http://www.orbitmotionsystems.com., Operation Manual PacDrive Robot D2, Edition 2008.
[109] S.,Briot, and I.,A. Bonev: Are parallel robots more accurate than serial robots. T. Can. Soc. Mech. Eng., **31**, 445–455, (2007).
[110] T.,Huang, Z.,Li, M.,Li, D.,Chetwynd, C.,M.,Gosselin: Conceptual design and dimensional synthesis of a novel 2DOF translational parallel robot for pick-and-place operations. ASMEJ. Mech. Des., **126**, 449–455, (2004).
[111] D., Zhang, C.,M., Gosselin,: Kinetostatic modeling of parallel mechanisms with a passive constraining leg and revolute actuators. Mech. Mach. Theory, **37**, 599–617, (2002).
[112] Q., Xu, Y., Li: An investigation on mobility and stiffness of a 3-DOF translational parallel manipulator via screw theory. Robot Comput. Integr. Manuf., , **24**, 402–414, (2008).
[113] S., Liu, T., Huang, J., Mei, et al.: Optimal design of a 4-DOF SCARA type parallel robot using dynamic performance indices and angularconstraints. J. Mech. Robot., **4**, (2012).
[114] Z., Huang, Y., Cao: Property identification of the singularity loci of a class of Gough-Stewart manipulators. Int. J. Robot. Res., **24**, 675–685, (2005).
[115] F., Pierrot, C., Reynaud, A., Fournier: Delta: A simple and efficient parallel robot. Robotica, **8**, 105–109, (1990).

[116] M., Neagoe, D., Diaconescu, R.,G., Săulescu: O nouă abordare a modelării preciziei structurilor de tip paralel. Partea I PRASIC '02, 169-170, (2002).

[117] J.,P., Merlet : Les robot parallèles Ed. Hermes, Paris, (1990).

[118] Aleshin, A., K., Glazunov, V.,A., Rashoyan, G.,V., and Offer Shai: Analysis of Kinematic Screws That Determine the Topology of Singular Zones of Parallel-Structure Robots. Journal of Machinery Manufacture and Reliability, **45**, 291–296, (2016).

[119] X, Kong, C.,M., Gosselin: Type synthesis of 3T1R 4-DOF parallel manipulators based on screw theory. IEEE Trans. Robot. Autom. **20**, 181–190, (2004).

[120] S., Guo, Y., Fang, H., Qu: Type synthesis of 4-DOF non overconstrained parallel mechanisms based on screw theory, Robotica, **30**, 31–37, (2012).

[121] Q., Xu, Y., Li,: An investigation on mobility and stiff-ness of a 3-DOF translational parallel manipulator via screwtheory, Robot Comput. Integr. Manuf. **24**, 402–414, (2008).

[122] X, Kong, C.,M., Gosselin: Type synthesis of 3-DOF translational parallel manipulators based on screw theory.J Mech Des **126**, 83–92,(2004).

[123] V., Glazunov: Twists of movements of parallel mechanisms inside their singularities, Mech. Mach. Theory, **41**, 1185–1195, (2006).

[124] R., Featherstone: Plucker Basis Vectors, Proc. IEEE ICRA, Orlando, FL, 1892–1897, (2006).

[125] A., Năstase: Mecanica Roboţilor. Mecanisme manipulatoare seriale. Galati University Press, (2012).

[126] G., Gogu: Structural Synthesis of Parallel Robots-Springer, Netherlands, (2008)

[127] Tsai, L.-W.: Robot Analysis - The Mechanics of Serial and Parallel Manipulators, John Wiley & Sons, (1999).

[128] G., Gogu: Structural synthesis of fully-isotropic translational parallel robots via theory of linear transformations Eur. J. Mech. A Solid, **23**, 1021–1039, (2004).

[129] P., Donelan: Singularity-theoretic methods in robot kinematics, Robotica, **25**, 641–659, (2007).

[130] M., Valasek, Z., Sika, V., Bauma et al.: Tractable treatment of design by multiobjective optimization –parallel kinematics case study, Multi. Syst. Dyn. 13, 143–174, (2005).

[131] Y., Lou, G., Liu, N., Chen et al.: Optimal design of parallel manipulators for maximum effective regular workspace, Proceedings of the IEEE / RSJ IROS 2005, 795–800, (2005).

[132] Y., Lou, G., Liu and Z., Li: Randomized optimal design of parallel manipulators, IEEE T. Autom Sci. Eng., **5**, 223–233, (2008).

[133] A., M., Hay and J., A., Snyman: Methodologies for the optimal design ofparallel manipulators, Int. J. Numer. Meth. Eng., **59**, 131–152, (2004).

[134] E., Ottaviano and M., Ceccarelli: Optimal design of CAPAMAN (Cassino Parallel Manipulator) with prescribed workspace, 2nd Workshop on Computational Kinematics KC 2001 Seoul, 35–43, (2001).

[135] F., Hao and J.,-P., Merlet: Multi-criteria optimal design of parallel manipu-lators based on interval analysis, Mech. Mach. Theory, **40**,157–171, (2005).

[136] H., Li, Z., Yang and T., Huang: Dynamics and elasto-dynamics optimizationof a 2-dof planar parallel pick and place robot with flexible links, Struct. Multidiscip. O. Journal, **38**, 195–204, (2009).

[137] I., A., Bonev: *Geometric Analysis of Parallel Mechanisms*. PhD thesis, Faculté des Sciences et de Génie, Université de Laval, (2002).

[138] B., M., St-Onge and C., M., Gosselin: Singularity analysis and representation of the general Gough-Stewart platform, Int. J. Rob. Res., **19**, 271–288, (2000).

[139] H., Li, C.,M., Gosselin, M., J., Richard and B., M., St-Onge: Analytic form of the sixdimensional singularity locus of the general Gough-Stewart platform, ASME J. Mech. Design, **128**, 279–287, (2006).

[140] A., K., Dash, I., Chen, S., H., Yeo and G., Yang: Workspace generation and planning singularity-free path for parallel manipulators, Mech. Mach. Theory, **40**, 776–805, (2005).

[141] S., Sen, B., Dasgupta and A., K., Mallik: Variational approach for singularity-free pathplanning of parallel manipulators, Mech. Mach. Theory, **38**, 1165–1183, (2003).

[142] T., Yoshikawa,: Manipulability of robotic mechanisms, Int. J. Rob. Res., **4**, pp. 3–9, (1985).

[143] G., Gogu: *Structural Synthesis of Parallel Robots*, Springer, 271-273, (2008)

[144] J.,P., Merlet: *Parallel Robots*, Kluwer Academic Publishers, Norwell, MA, USA, ISBN 0792363086, (2006).

[145] J.,P., Merlet: Jacobian, manipulability, condition Number and Accuracy of parallel robots, J. Mech. Design, **128**, 199–206, (2006).

[146] R., Rodrigues dos Santos, S., Valder and P., S., Sezimária de Fátima: Multi-Criteria Optimal Path Planning of Flexible Robots, Ed. Küçük S., Serial and parallel robot manipulators – Kinematics, Dynamics, Control and Optimization, InTech., 344-345, (2012).

[147] T., Yoshikawa, Dynamic manipulability of robot manipulators, Trans. Soc. Instrum. Control Eng. **21** (1), 970–975, (1985).

[148] A., Bowling, O., Khatib : The dynamic capability equations: a new tool for analyzing robotic manipulator performance, IEEE Trans. Robot., **21** (1), 115–123, (2005).

[149] H., Shao, L., Wang, L., Guan, et al. : Dynamic manipulability and optimization of a redundant three DOF planar parallel manipulator, in: Proceedings of the ASME / IFToMM International Conference on Reconfigurable Mechanisms and Robots, 302–308, (2009).

[150] P., Ogbobe, H., Jang, J., He, C., Yang, J., Han : Analysis of coupling effects on hydraulic controlled 6 degrees of freedom parallel manipulator using joint space inverse mass matrix in: Proceedings of the Second International Conferences on Intelligent Computation Technology and Automation, 845–848, (2009).

[151] Y. Yao, S. Fu, L. Han, Block diagonal dominance analysis and judgment of Stewart platform's joint-space inertia matrix, Chin. J. Mech. Eng., **44** (6), 101–106, (2008).

[152] A. Codourey, Dynamic modeling and mass matrix evaluation of the DELTA parallel robot for axes decoupling control, in: Proceedings of the IEEE/RSJ International Conference on Intelligent Robots and Systems, Osaka, Japan, 1211–1218, (1996).

[153] T., Huang, J., Mei, Z., Li, X., Zhao : A method for estimating servomotor parameters of a parallel robot for rapid pick-and-place operations, Trans. ASME, **127** (4), 596–601, (2005).

[154] Z., F., Shao, X., Tang, X., Chen, L., P., Wang : Inertia match of a 3-RRR reconfigurable planar parallel manipulator, Chin. J. Mech. Eng. **22** (6), 791–799, (2009).

[155] Z., F., Shao, X., Tang, X., Chen, et al. : Research on the inertia matching of the Stewart parallel manipulator, Robot. Comput.-Integr. Manuf., **28** (6), 649–659, (2012).

[156] S., Bhattacharya, D., N., Nenchev, M., Uchiyama: A recursive formula for the inverse of the inertia matrix of a parallel manipulator, Mech. Mach. Theory**, 33** (7), 957–964, (1998).

[157] C., M., Gosselin: Parallel computationnal algorithms for the kinematics and dynamics of parallel manipulators. IEEE Int. Conf. Robot. Autom. **1**, 883–889 New York, (1993).

[158] G., Lebret, G., K., Liu, F., L., Lewis : Dynamic analysis and control of a Stewart platform manipulator. J. Robot. Syst., **10** (5), 629–655 (1993).

[159] K., M., Lee, D., K., Shah: Dynamic analysis of a three-degrees-of-freedom in-parallel actuated manipulator. IEEE J. Robot. Autom., **4** (3), 361–368 (1988).

[160] M.-J., Liu, C.-X., Li, C.-N., Li: Dynamics analysis of the Gough–Stewart platform manipulator. IEEE Trans. Robot. Autom. **16** (1), 94–98, (2000).

[161] A., Codourey, E., Burdet: A body oriented method for finding a linear form of the dynamic equatiojns of fully parallel robot. IEEE Conf. on Robotics and Automation, 1612–1619. Albuquerque, New Mexico, U.S. (1997).

[162] W., Khalil, O., Ibrahim : General solution for the dynamic modeling of parallel robots, J. Intell. Robot. Syst.: Theory Appl. **49** (1) 19–37, (2007).

[163] Z. F. Shao, X. Tang, L.P. Wang, et al., Dynamic modeling and wind vibration control of the feed support system in FAST, Nonlinear Dyn., **67** (2), 965–985, (2012).

[164] Z., F., Shao, X., Tang, L., Wang : Dynamics verification experiment of the Stewart parallel manipulator, Int. J. Adv. Robot. Syst. **12**, (2015).

[165] B., Dasgupta, T., S., Mruthyunjaya: Closed-form dynamic equations of the general Stewart platform through the Newton–Euler approach. J. Mechanism and Machine Theory **33** (7), 993–1012, (1998).

[166] B., Dasgupta, T., S., Mruthyunjaya: A Newton–Euler formulation for the inverse dynamics of the Stewart platform manipulator. J. Mech. Mach. Theory, **33** (8), 1135–1152, (1998).

[167] Dasgupta, B., Choudhury, P.: A general strategy based on the Newton–Euler approach for the dynamic formulation of parallel manipulators. J. Mech. Mach. Theory, **34** (6), 801–824 (1999).

[168] H. Pang, M. Shahinpoor, Inverse dynamics of a parallel manipulator, J. Robot. Syst., **11** (8), 693–702, (1994).

[169] S., Staicu : Dynamics of the 6-6 Stewart parallel manipulator, Robot. Comput.Integr. Manuf. **27** (1), 212–220, (2011).

[170] J., Ginsberg: Engineering Dynamics, Cambridge University Press, 2008.

[171] W., Khalil, E., Dombre: Modeling, Identification and Control of Robots. London: Hermes Penton (2002).

[172] Z., F., Shao, X., Tang, L., P., Wang : Optimum design of 3-3 Stewart platform considering inertia property, Adv. Mech. Eng., **5,** 1–10, (2013).

[173] Y., Zhao, F., Gao, Inverse dynamics of the 6-dof out-parallel manipulator by means of the principle of virtual work, Robotica, **27,** 259–268, (2009).

[174] L.-W., Tsai: Solving the inverse dynamics of a Stewart–Gough manipulator by the principle of virtual work. J. Mech. Des., **122**, 3–9 (2000).

[175] S., Dubowsky, F., Freudenstein : Dynamic Analysis of Mechanical Systems with Clearances, Part 1: Formulation of Dynamic Model, ASME J.Eng. Ind., **93**, 305–309, (1971).

[176] F., Farahanchi, S., W., Shaw: Chaotic and Periodic Dynamics of a Slider-Crank Mechanism with Slider Clearance, J. Sound Vib., **177**, 307–324, (1994).

[177] J., Rhee, A., Akay: Dynamic Response of a Revolute Joint With Clearance," Mech. Mach. Theory, **31**, 121–134, (1996).

[178] P., Flores, J., Ambrósio and J., P., Claro: Dynamic Analysis for Planar Multibody Mechanical Systems with Lubricated Joints, Multibody Syst.Dyn., **12**, 47–74, (2004).

[179] H., M., Lankarani and P., E., Nikravesh: A Contact Force Model With Hysteresis Damping for Impact Analysis of Multibody Systems," ASME J. Mech. Des., **112**, 369–376, (1990).

[180] J., A., Ambrósio: Impact of Rigid and Flexible Multibody Systems: Deformation Description and Contact Models, *Virtual Nonlinear Multibody Systems*, NATO Advanced Study Institute, W. Schiehlen and M. Valásek, eds.,Plenum, New York, **2**, 15–33, (2002).

[181] M., A., Brown: A Deployable Mast for Solar Sails in theRange of 100-1000 m, ASR, **48**, 1747-1753, (2011).

[182] Z., H., Qi, Y., S., Xu, X., M., Luo and S., J., Yao: Recursive Formulations for Multibody Systems with Frictional Joints Based on the Interaction Between Bodies, Multibody Syst. Dyn., **24**, 133-166, (2010).

[183] C., S., Liu, K., Zhang and L., Yang: Normal Force-Displacement Relationship of Spherical Joints with Clearances, J. Comput. Nonlin. Dyn., **1**, 160-167, (2006).